Journal of
Medicinal Chemistry

Article

Design, Synthesis and Pharmacological Evaluation of Potent Positive Allosteric Modulators of the Glucagon-like Peptide-1 Receptor (GLP-1R)

Maria Mendez, Hans Matter, Elisabeth Defossa, Michael Kurz, Sylvain Lebreton, Ziyu Li, Matthias Lohmann, Matthias Loehn, Hartmut Mors, Michael Alois Linus Podeschwa, Nils Rackelmann, Jens Riedel, Pavel Safar, David Thorpe, Matthias Schaeffer, Dietmar Weitz, and Kristin Breitschopf

J. Med. Chem., **Just Accepted Manuscript** • DOI: 10.1021/acs.jmedchem.9b01071 • Publication Date (Web): 09 Oct 2019

Just Accepted

is published by the American Chemical Society. 1155 Sixteenth Street N.W., Washington, DC 20036

Design, Synthesis and Pharmacological Evaluation of Potent Positive Allosteric Modulators of the Glucagon-like Peptide-1 Receptor (GLP-1R)

María Méndez, Hans Matter*, Elisabeth Defossa, Michael Kurz, Sylvain Lebreton[§], Ziyu Li, Matthias Lohmann, Matthias Löhn, Hartmut Mors, Michael Podeschwa, Nils Rackelmann, Jens Riedel, Pavel Safar[§], David S. Thorpe[†], Matthias Schäfer, Dietmar Weitz, Kristin Breitschopf*

Sanofi-Aventis Deutschland GmbH, Industriepark Höchst, 65926 Frankfurt, Germany.

[§]Current address: Icagen, 2090 E Innovation Park Drive, Oro Valley, AZ 85755, USA.

†Current address: University of Arizona, Clinical Sciences & Translational Medicine Division of Cardiology, Dept of Medicine, Sarver Heart Center, 1501 N Campbell Ave. Tucson, AZ 85724, USA

Abstract

The therapeutic success of peptidic GLP-1 receptor agonists for treatment of type 2 diabetes mellitus (T2DM) motivated our search for orally bioavailable small molecules that can activate the GLP-1 receptor (GLP-1R) as a well-validated target for T2DM. Here, the discovery and characterization of a potent and selective positive allosteric modulator (PAM) for GLP-1R based on a 3,4,5,6-tetrahydro-1H-1,5-epiminoazocino[4,5-b]indole scaffold is reported. Optimization of this series from HTS was supported by a GLP-1R ligand binding model. Biological *in-vitro* testing revealed favorable ADME and pharmacological profiles for the best compound **19**. Characterization by *in-vivo* pharmacokinetic and pharmacological studies demonstrated that **19** activates GLP-1R as positive allosteric modulator (PAM) in presence of the much less active endogenous degradation product GLP1(9-36)NH_2 of the potent endogenous ligand GLP-1(7-36)NH_2. While these data suggest the potential of small molecule GLP-1R PAMs for T2DM treatment, further optimization is still required towards a clinical candidate.

Introduction

The glucagon-like-peptide-1 receptor (GLP-1R), a class B G protein-coupled receptor (GPCR), is a well-validated target for the treatment of type 2 diabetes mellitus (T2DM).[1,2,3] Several peptidic GLP-1R agonists from the class of incretin mimetics, such as exenatide, liraglutide, lixisenatide, albiglutide and dulaglutide, are approved today for treatment of T2DM.[4,5,6] The therapeutic success of these injectable GLP-1 analogs prompted us and other groups to search for peptide variations or small molecules that act as GLP-1R agonist or positive allosteric modulators (PAMs) leading to similar pharmacodynamic effects. PAMs could have the potential for producing reduced side-effects such as nausea and vomiting prevalent in injectable GLP-1R agonists, which in turn limits their maximal efficacy. Thus, orally administered PAMs would likely result in higher patient convenience and compliance with maximal therapeutic efficacy.[7,8,9,10,1112]

The search for small molecular entities able to directly activate the GLP-1R is ongoing for many years since mimicking the large interaction surface area involved in endogenous peptide ligand binding to class B GPCRs is challenging. Two main approaches have been pursued for activation of GLP-1R with small molecules, namely searching for direct agonists, or for positive allosteric modulators (PAMs) able to enhance the activity of either the endogenous ligand GLP-1(7-36)NH_2 or its much less active degradation product GLP1(9-36)NH_2, which lacks the first two amino acids His7 and Ala8.[13,14] PAMs do not to interfere with endogenous peptide levels and are expected not to induce tachyphylaxis, which could be an advantage against full agonists.

Some of the earlier reported small molecule GLP-1R direct agonists suffer from non-drug-like properties, such as high lipophilicity and molecular weight, which causes low plasma exposure after oral administration.[15,16,17] The most advanced compound is TTP273 from vTv

Therapeutics, which is to our knowledge in clinical development for treatment of T2DM (Phase 2 completed).[18] Although the chemical structure of TTP273 has not been disclosed, dioxino-2,3-isoquinoline derivatives, such as **1** (Figure 1) have been disclosed by Transtec (now vTv-Therapeutics) in the patent literature.[19,20] As expected for a small molecule with these mentioned characteristics, considerable formulation efforts and high doses of TTP273 were necessary to conduct clinical trials.[21] More recently, Pfizer and Lilly have also disclosed small molecule GLP-1R agonists in clinical development (PF-06882961[22] and OWL833[23,24] in-licenced from Chugai), although structures have not yet been reported, they might be related to those disclosed in the patent literature (compounds **7** and **8**).[25,26] Current data suggest that some of the drawbacks from earlier molecules might have been overcome.

The best-characterized GLP-1R PAMs (BETP (**2**) and compound 2 (**3**), Figure 1) act by covalently modifying a cysteine side chain in the GLP-1R, inducing thereby a conformational change of the receptor which is able to trigger the GPCR signal cascade upon addition of less active GLP1(9-36)NH_2.[27,28] However, the presence of reactive chemical functionalities in both molecules **2** and **3**, and the fact that these two compounds besides their PAM effect also show direct agonistic activity on their own (they are allo-agonists),[29] precludes them from being good *in-vivo* tools for validating the potential of the solely positive modulation approach in a T2DM-relevant disease context. Although several non-covalent compounds have been reported as PAMs for the GLP-1R (compounds **4**, **5** and **6** in Figure 1), only limited information about their *in-vivo* pharmacology in T2DM disease-models is currently available.[30,31,32,33] Given that GLP1(9-36)NH_2 accounts for ca. 80-90% of the postprandrial GLP-1 total concentration in humans[34] and that its half live in vivo is approximately five times higher than the active GLP1(7-36)NH_2 counterpart, we hypothesized that enhancing the activity of the peptide ligand GLP1(9-36)NH_2 could result in a therapeutic valuable approach. In order to increase our success chances, we conducted a HTS campaign with two

different experimental settings with the aim to identify both small molecule direct agonists and PAMs for the GLP-1R. Unfortunately, this approach did not yield interesting starting points as small molecule direct agonists which would justify a chemical optimization program.

However, the HTS outcome analysis led to the discovery and characterization of a potent and selective positive allosteric GLP-1R modulator based on a 3,4,5,6-tetrahydro-1H-1,5-epimino-azocino[4,5-b]indole scaffold (see Figure 2). This promising series was then chemically optimized and we were able to show that the most potent compound and its analogues indeed activate the GLP-1R as PAMs in combination with the endogenous ligand GLP1(9-36)NH_2.

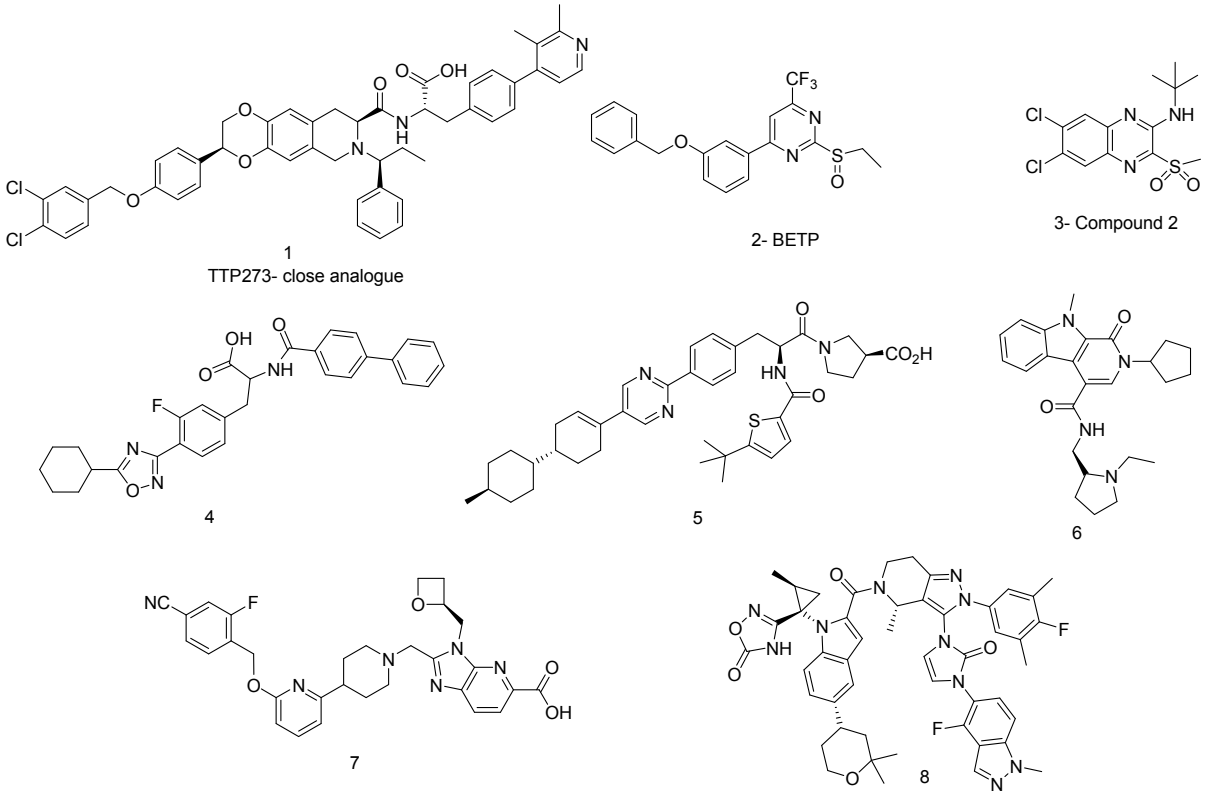

Figure 1. Small molecule GLP-1R agonists and allosteric modulators in literature.

Results and discussion

Discovery of GLP-1R PAMs

We performed a HTS of the Sanofi compound collection to identify positive allosteric modulators for the endogenous ligand GLP1(9-36)NH_2 to interact with the GLP-1R. This was done using an HTRF cAMP assay in a HEK293 cell line overexpressing the human GLP-1R. In this assay, both GLP-1(7-36)NH_2 and GLP1(9-36)NH_2 peptides activate the GLP-1 receptor, albeit with significantly different potencies. The EC_{50} value of the GLP-1(7-36)NH_2 is approximately 10,000-fold better than the EC_{50} value for the GLP1(9-36)NH_2. When performing the screening assay, all compounds were tested at the EC_{20} concentration of the orthosteric ligand GLP1(9-36)-NH_2 to better assess the potentiation of putative HTS-hits. Subsequently, compounds were tested for their ability to shift the EC_{50} value of the endogenous GLP1(9-36)NH_2 at fixed compound concentrations of 10 and 3 μM, thereby aiming to demonstrate improved biological action of the less active endogenous peptide. Among the several active compounds from HTS, there were many with potentially reactive chemical functionalities (not shown). Consequently, a glutathione (GSH) stability assay served to focus on chemotypes able to activate GLP-1R in a non-covalent manner. Such a stability assay is used as counterscreen to detect substances with electrophilic moieties leading to covalent modification of nucleophiles.

One chemical series based on the 3,4,5,6-tetrahydro-1H-1,5-epiminoazocino[4,5-b]indole scaffold showed a particularly high activity in our HTS assay (compound **8**, PAM EC_{50} 600 nM/100% efficacy, see table 1). The best compound exhibited a very significant effect in enhancing (shifting) the EC_{50} value of GLP1(9-36)NH_2 (> 500 times @ 10 μM). In the orthologue mouse receptor assay, which served as *in-vitro* surrogate for our *in-vivo* model, the biological activity was similar or slightly improved (PAM EC_{50} 300 nM/100%). This chemical series originated from a synthesized chemical library based on natural-product-like

scaffold using a Pictet-Spengler intramolecular cyclization.[35] This origin allowed for rapid structure-activity-relationship (SAR) evaluation due to the internal availability of numerous analogues plus a reasonable access to new derivatives by parallel-synthesis chemistry for further exploring the SAR. Although the hit structure **8** is clearly outside of the property range commonly assigned to lead-like structures from HTS (MW: 585.6),[36] its robust biological activity encouraged us to optimize this motif. Hit structures were always obtained as single enantiomers and we could rapidly determine that the S,S stereochemistry at the bridgehead carbon atoms is necessary for high GLP-1R activity in our primary assay. The corresponding R,R isomers provided minor 2-4 EC_{50} shifts for GLP1(9-36)NH_2. Other isomers were not tested.

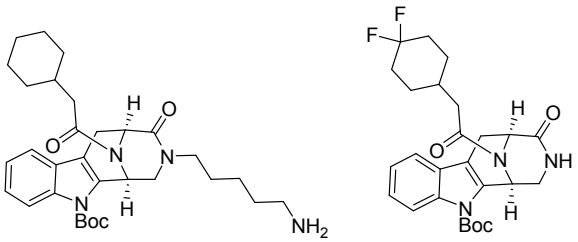

Figure 2. Structure of HTS hit **(8)** and advanced hit **(9).**

Chemistry

Synthesis of these compounds starts with the amide coupling of Z-protected N-Boc L-tryptophan **9a** (Scheme 1) and a diacetal-containing amine of the type **10** under standard EDC-coupling conditions. The subsequent stereospecific Pictet-Spengler intramolecular cyclisation in the presence of formic acid then delivered the polycyclic scaffold **12**, mostly with partial deprotection of the Boc-group at the indole-N1 moiety. A two-step protection /

deprotection protocol was established with crude mixtures to deliver the mono-Boc-protected intermediate **12**, which was then submitted to standard deprotection conditions of the Z-group. Final amide coupling reaction with 2-(4,4-difluorocyclohexyl)-acetic acid rendered compound **9** in good yields and as single (S,S) enantiomer. Subsequent functionalization of the amide nitrogen of compound **9** was performed via a Michael addition with acrolein and subsequent addition of MeMgBr, which delivered compound **14** as a 1:1 mixture of two

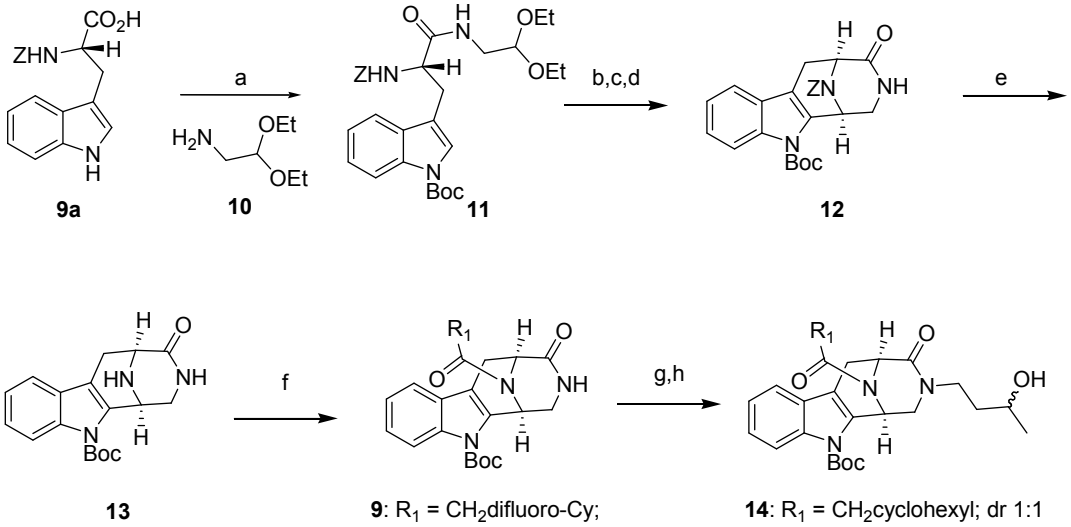

diastereomers.

(a) EDC, Oxyma, DMAP, N-methyl morpholine, DMF, rt, 74%; Then DMAP, Boc_2O, MeCN, 45%. (b) HCO_2H, rt, 80%. (c) Boc_2O, CH_3CN, DMAP, rt. (d) HCO_2H, rt. (e) H_2, Pd/C, MeOH, rt, 90%. (f) R_2CO_2H, EDC, Oxyma, DMAP, N-methyl morpholine, DMF, rt, 75%. (g) Acrolein, NaOH, THF (h) MeMgBr, THF, 27% over two steps, dr 1:1.

Scheme 1. Synthesis of compounds **9** and **14**.

For the synthesis of compound **19**, a slightly modified synthesis was employed as shown in Scheme 2. Starting from the Fmoc-protected tryptophan **9b** and the amine building block

15,[37] intermediate **16** was obtained via HATU coupling. Oxidation of the alcohol with Dess-Martin periodinane and subsequent *in-situ* cyclisation of the crude reaction mixture led to polycyclic intermediate **17**, which was submitted to Fmoc-deprotection using $MeNH_2$ to render intermediate **18** as a mixture of diastereomeres, which could be separated at this stage via HPLC. Final coupling with 2-(4,4-difluorocyclohexyl-)acetic acid and subsequent ester hydrolysis delivered compound **19** as a single enantiomer. The relative stereochemistry of **19** could be unambiguously assigned by characterization and complete structure elucidation of intermediate **18** by NMR spectroscopy (see supporting information).

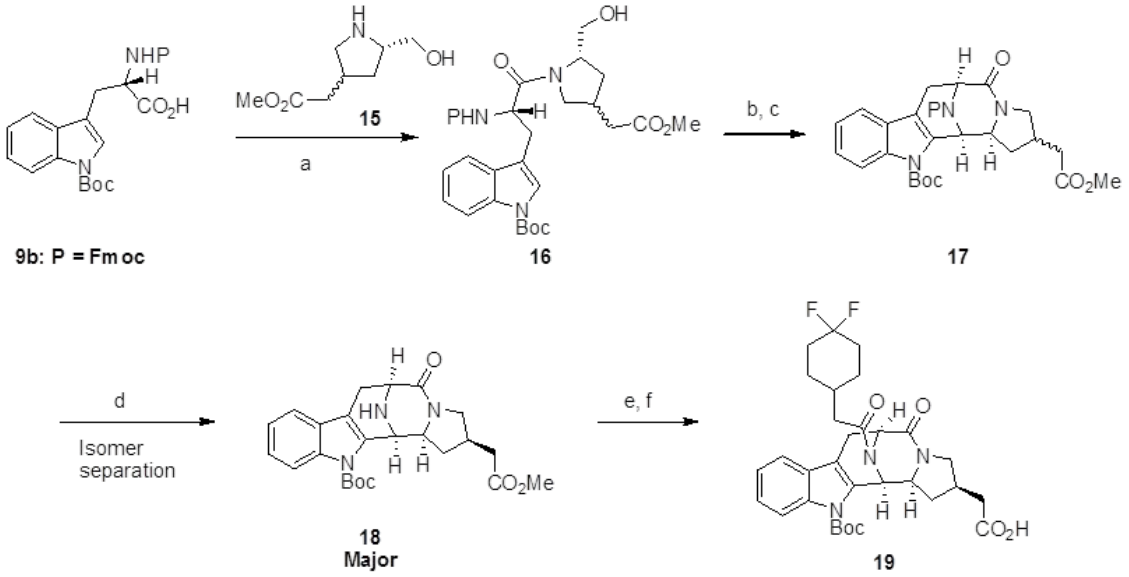

(a) HATU, DIPEA, THF , rt, 37%; (b) Dess-Martin, CH_2Cl_2, rt, 40% ; c) H_2CO_2H, rt, 45%. (d) Me_2NH, THF, rt, 72%; (e) 2-(4,4-difluorocyclohexyl-)acetic acid, HATU, DIPEA, THF , rt; (f) LiOH, MeOH:H_2O, rt (38% over two steps).

Scheme 2. Synthesis of compound **19**.

Molecular pharmacology

Starting from the HTS hit **8**, we first aimed to identify a simplified chemical analog retaining biological activity in our assay, which led to identification of compound **8** (table 1). This new

molecule lacks the non-drug like basic side chain but was more active in the primary PAM assay (EC_{50} / E_{max} 5 nM / 100%). Furthermore it shifted the EC_{50} value from GLP1(9-36)NH_2 by a factor of 3,791 at 10 µM and 1,183 at 3 µM, maintaining full agonistic efficacy (E_{max} 100%). For this and other compounds in this study, relevant data are summarized in table 2. Compound **8** is a specific ligand for GLP-1R without significant activity in the cAMP accumulation assay with the parental, GIP-receptor (gastric inhibitory polypeptide), human VIPR2 (vasoactive intestinal peptide receptor 2) or glucagon receptor overexpressing cell lines, and it was also found to be highly stable in the GSH assay.

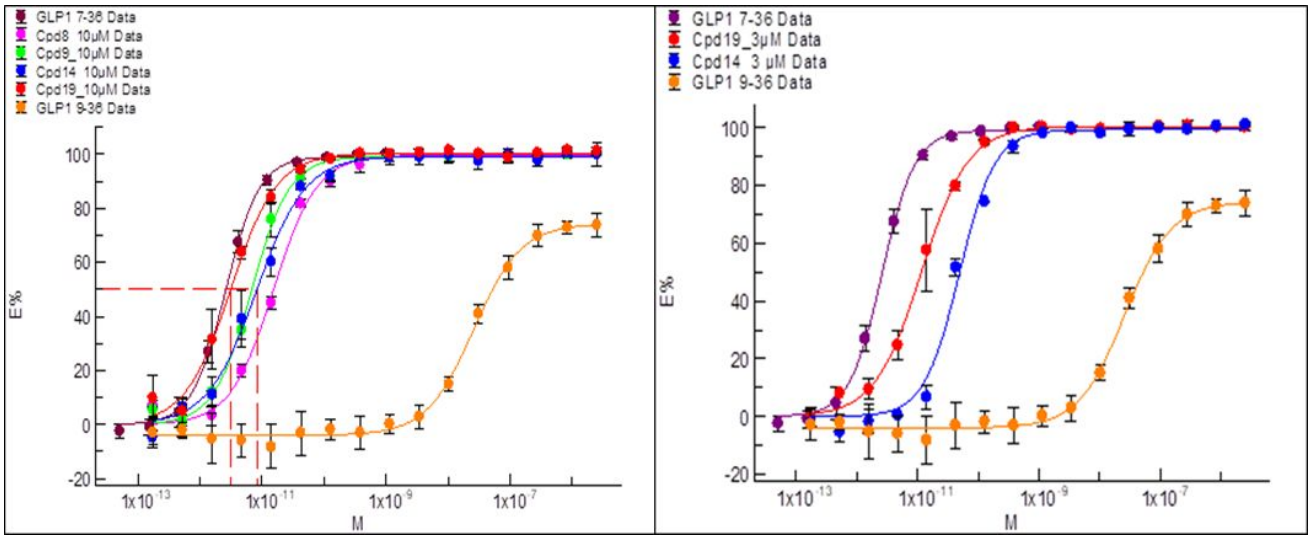

Figure 3. Dose-response curves from functional *in-vitro* assay data for cAMP response of GLP-1(7-36)NH_2 and GLP1(9-36)NH_2 with or without test compounds in PSC-HEK293 cells overexpressing GLP-1R using the shift assay format. Left: 10 µM compound concentration. Right: 3 µM compound concentration.

Table 1: Summary of in vitro data for compounds 8-19. a) Compound EC_{50} at EC_{20} of GLP1(9-36)NH2 in the cAMP response assay in PSC-HEK293 cells b) Shift factors of GLP1(9-36)NH_2 EC_{50} for compound concentrations of 10 and 3 µM in cAMP response assay in the PSC-HEK293 c) Compound EC50 at EC20 of GLP1(9-36)NH2 in the cAMP response

assay in 1.1B4 cells d) Compound effect on high glucose-mediated Ca^{2+} influx in Min6 beta-cells @ 10 µM vs. HG control (FLIPR assay) e) OK = No direct effect on cAMP in parental HEK293 cells, HEK293 cells overexpressing GLP-1R, GCGR, VIPR or GIPR; no modulation of cAMP response to GLP-1(7-36)NH_2 or oxyntomodulin in GLP1R overexpressing HEK293 cells, or to GLP-1(9-36)NH_2 in GCGR overexpressing HEK293 cells.

ID	PAM EC_{50} [µM] / Emax [%]	EC_{50} Shift		1.1B4 cells PAM EC_{50} [µM] / Emax [%]	Fold change Ca^{2+} Influx b)	Selectivity c)
		10 µM	3 µM			
Cpd 8	0.6 / 91%	1,681	nda)	nd		
Cpd 9	0.005 / 99%	3,795	nda)	nd	nd	nd
Cpd 14	0.0015 / 100%	3,143	526	0.04 / 100	0.9	OK
Cpd 19	0.005 / 100%	8,188	2,215	0.130/102%	1.2	OK

It is also a selective potentiator of GLP-1R in the presence of the GLP1(9-36)NH_2 since it neither induced a cAMP signal in the corresponding recombinant cell line when tested alone nor in the presence of 10 nM GLP-1(7-36)NH_2 or oxyntomodulin (data not shown). Furthermore, in a radioactive ligand binding assay, compound **9** was not able to displace the radioactive labelled peptide GLP-1(7-36)NH_2, thus supporting our presumed allosteric mode of action. Compound **9** was also selective against other common channels and receptors. When investigating in a standard receptor (CEREP-33 panel[38]) and ion channel antitarget panel, only moderate agonistic effects on the K_{ATP} channel (EC_{50} 2.67 µM) and minor effects on ion-channels such as $N_{av}1.2$ and $N_{av}1.5$ were observed.[39]

However, when testing this compound for its ability to shift the EC_{50} value of GLP1(9-36)NH_2 in the human pancreatic 1.1B4 β-cell line, which endogenously expresses the GLP-1 receptor, no EC_{50} value shift was observed. As shown in Figure 4, the ligand GLP1(9-36)NH_2 alone does not exhibit any activity on the endogenously expressed GLP-1R, whereas GLP-1(7-36)NH_2 clearly activates its natural receptor.

Further optimization of the HTS hits led to analogues **14** and **19**, bearing both a polar substituent at the amide nitrogen. Our homology model (see below) suggested that a potential polar interaction to Lys190 might be beneficial for potency. Interestingly, these compounds could clearly potentiate GLP1(9-36)NH_2 in our *in-vitro* assay (see table 1). In this primary PAM assay, both compounds showed a similar potency (EC_{50} / E_{max} 1.5 nM / 100% for compound **14** and 5 nM / 100% for compound **19**). However, **19** showed superior activity in the primary assay by shifting the EC_{50} value of GLP1(9-36)NH_2 compared to **14** (8188 / 2215 fold at 10 and 3 μM for **19** versus 3143 / 526 fold at 10 and 3 μM for **14**). To our knowledge, this is the best potentiation ability described for a non-covalent PAM of the GLP-1R reported so far.[40] Moreover, in the endogenous human pancreatic β-cell line 1.1B4, both compounds **14** and **19** showed robust PAM efficacy, although the difference between these two compounds was not as pronounced as observed previously in the overexpressing cell line (Figure 4).

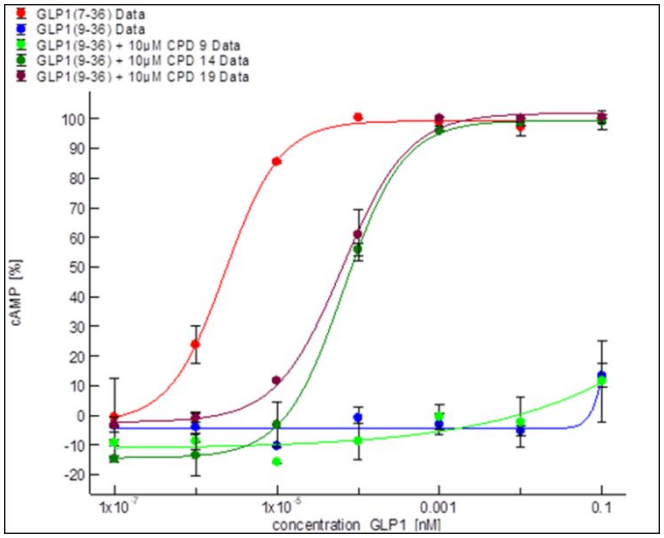

Figure 4. Dose-response curves from functional *in-vitro* assay for cAMP response of GLP-1(7-36)NH_2 and GLP1(9-36)NH_2 with or without test compounds in human pancreatic 1.1B4 cells using the shift assay format.

Both compounds **14** and **19** also proved to be selective potentiators of GLP1(9-36)NH_2. They did neither alter the biological responses of GLP-1(7-36)NH_2 nor of oxyntomodulin in the recombinant cell line system (data not shown). Furthermore, they had no effect on cAMP accumulation, when tested alone in HEK293 cells overexpressing the GLP-1R, in the parental cell line or in HEK293 cells overexpressing the glucagon receptor either alone or in the presence of GLP1(9-36)NH_2. Additional assays were performed using cells overexpressing the human GIP-receptor and the human VIPR2. Both compounds were found inactive, when tested tested for agonistic activity and for their effect as allosteric modulator using GLP1(9-36)NH_2, GIP.[41]

The good selectivity displayed by both compounds in our standard receptor and ion channel panels and against other typical diabetes-relevant GPCRs, such as TGR5 or GPR119 (see supporting information for full data), prompted us to investigate these compounds in relevant

functional assays like the glucose-stimulated insulin secretion (GSIS) assay in dispersed rat and mouse pancreatic islets.

As shown in Figure 5, compound **14** significantly improved the GLP1(9-36)NH_2-mediated glucose-stimulated insulin secretion in dispersed rat pancreatic islets. This GSIS potentiation effect was much more pronounced at higher concentrations of the peptide ligand. However, when higher concentrations (10 μM) of compound **14** were tested, its ability to potentiate the effect of 10 nM GLP1(9-36)NH_2 vanished and even turned into an inhibitory effect in the absence of the peptide ligand GLP1(9-36)NH_2 (Figure 5b).[42] In contrast, compound **19** showed a distinct behavior in this assay. It robustly stimulated GSIS in dispersed rat pancreatic islets even at high concentration (10 μM) in the presence of 10 nM GLP1(9-36)NH_2 to an extent, which is comparable to the positive control (10 nM GLP-1 (7-36)NH_2) (Figure 4c). Moreover, when tested alone, it did not show any inhibitory effect. It is important to note, that the insulinotropic response in this assay was absent at low glucose concentrations (see supporting information for details).

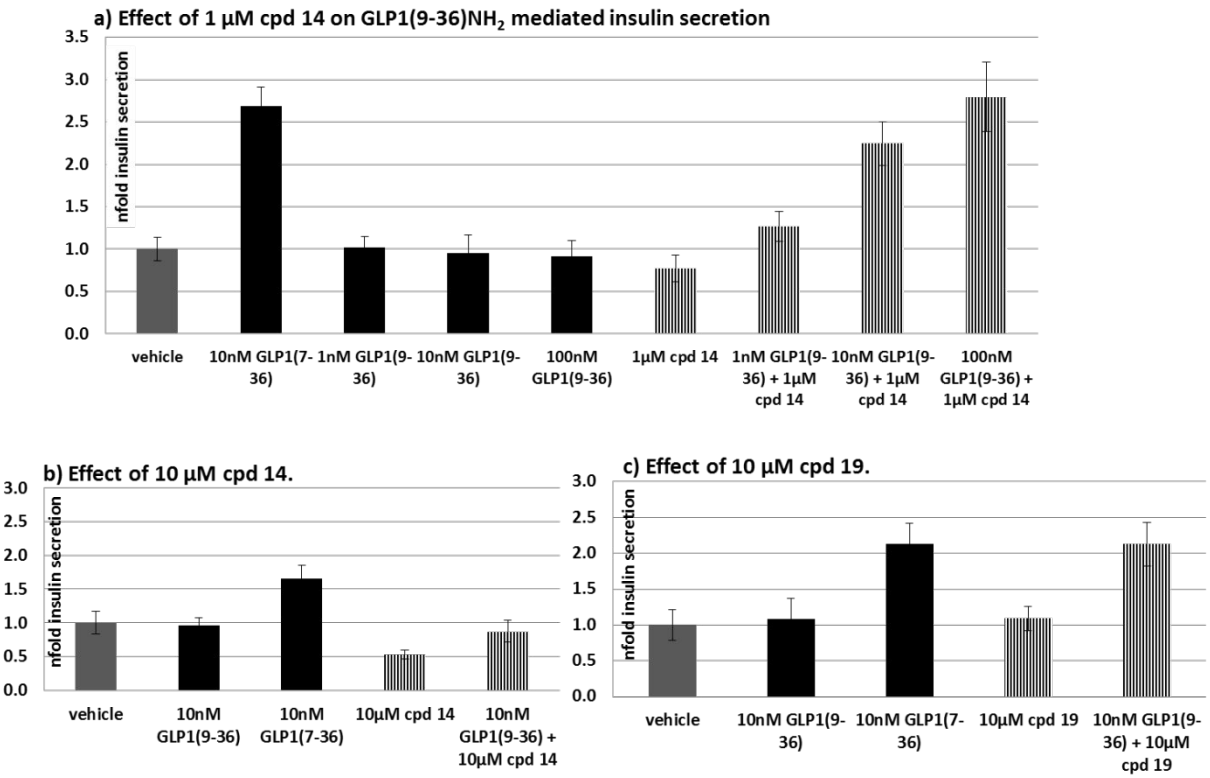

Figure 5. Glucose-stimulated insulin secretion (GSIS) from dispersed rat islets for PAM-compounds **14** (a, b) and **19** (c). Dispersed islets were incubated with high (15 mM) glucose in the presence of vehicle control (DMSO) +/- respective compound (1 µM) or GLP-1 ligand (1/10/100 nM) +/- respective compound (1 µM). Diluent for GLP-1 ligand was DMSO. N ≥ 9 / condition. **p ≤ 0.001 vs. respective control; ****p ≤ 0.00001 vs. respective control. For b) and c), incubation was done +/- respective compound (10 µM) or GLP-1 ligand (10 nM) +/- respective compound (10 µM).

To investigate whether the inhibitory effect on the glucose-stimulated insulin secretion observed with compound **14** at high concentration is an effect, which is not mediated by GLP-1R, we tested **14** in mouse islets derived from GLP-1R(-/-) mice (Figure 6).[43] In this model, neither GLP-1(7-36)NH_2 nor GLP1(9-36)NH_2 induced the insulinotropic response either at low or high glucose. Compound **14** still displayed an inhibitory effect on the insulin

secretion, when tested in the presence or in the absence of GLP1(9-36)NH_2 in a magnitude comparable to the one observed in the rat islets. This finding suggests that the inhibitory mechanism for compound **14** is likely linked to an off-target effect.

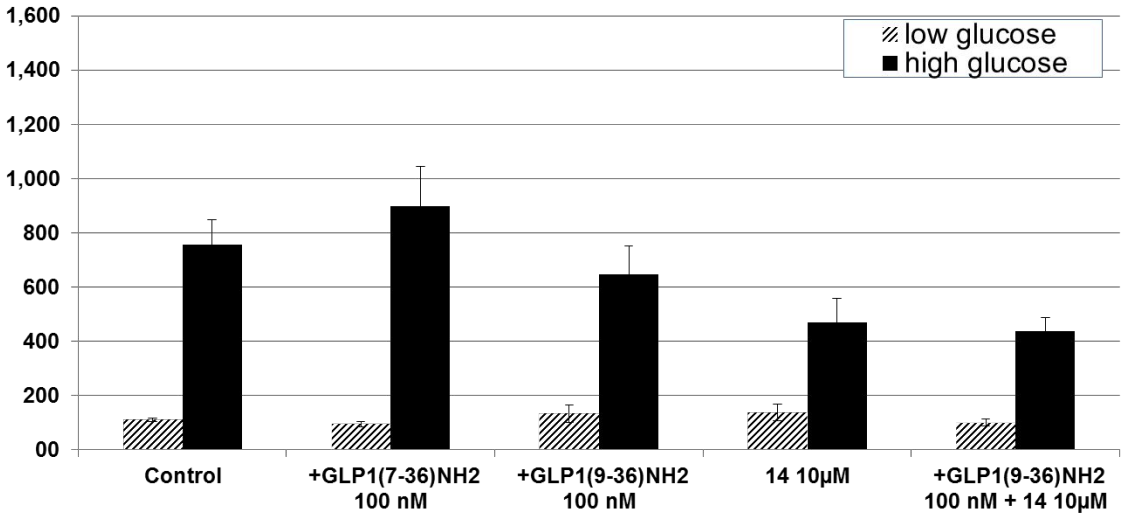

Figure 6. Effect on GSIS on islets of GLP-1(-/-) CD-1 mice. Dispersed mouse islets were incubated at low (3 mM) and high (15 mM) glucose with: 100 nM GLP-1(7-36)NH_2, 100 nM GLP1(9-36)NH_2; 10 µM compound **14** and 100 nM GLP1(9-36)NH_2 + 10 µM compound **14**.

As further selectivity testing of compound **14** did not reveal a single receptor or ion channel responsible for this inhibitory effect, we hypothesized that it was possibly due to a polypharmacology effect causing a counter-regulatory response in the insulin secretion pathway. Indeed, when testing the influence of compound **14** alone in a Ca^{2+} mobilization assay in the mouse pancreatic β-cell line Min6-c4, it blocked glucose-mediated Ca^{2+} influx in a similar manner as the known K_{ATP} opener diazoxide, suggesting a detrimental influence on metabolism-secretion coupling upstream of insulin granule exocytosis and independent of the GLP-1 pathway. This phenotypic high-throughput assay allowed us then to efficiently

exclude other compounds from further profiling that abrogated glucose-stimulated Ca^{2+} influx like compound **14**.

Indeed, as shown in Figure 7, compound **19** tested under similar conditions did not inhibit Ca^{2+} mobilization even at the highest concentration, prompting us to evaluate its potential in subsequent *in-vivo* studies.

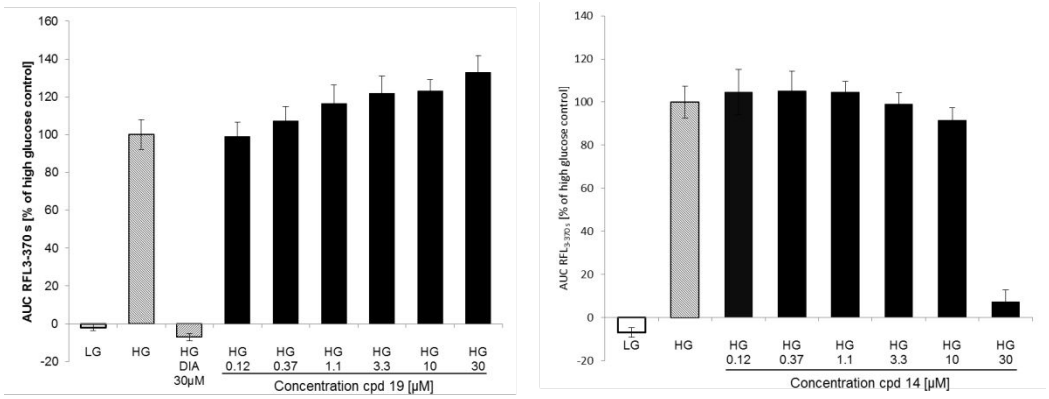

Figure 7. Effect of compounds **19** (left) and **14** (right) on Ca^{2+} mobilization. LG: Low glucose (2.5 mM); HG: high glucose (15 mM), DIA: K_{ATP} opener diazoxide.

Ligand binding mode hypothesis in GLP-1R

The X-ray structure of the full-length GLP-1R with a peptidic agonist (peptide 5 with modified GLP-1 residues 8-17, PDB 5NX2, resolution 3.7Å)[44] in the active conformation[45] was used to derive a binding hypothesis for the 3,4,5,6-tetrahydro-1H-1,5-epiminoazocino[4,5-b]indole scaffold. However, due to the lack of a co-crystal structure and dedicated GLP-1R mutants, this is only a hypothesis to illustrate our reasoning for ligand optimization, while other potential binding modes for this series cannot be excluded.

The following arguments suggest that our series binds to a region overlapping with the orthosteric pocket: 1) The ligands exhibit a positive allosteric effect with addition of the

truncated peptide GLP1(9-36)NH_2, but not in the presence of the full GLP-1(7-36)NH_2 with amino acids His7-Ala8 close to the orthosteric site, thereby blocking the entrance into this area; 2) activation of GLP-1R is only possible by contacting both the ECD with the truncated GLP-1 peptide derivative and the 7TM domain; 3) the binding site hypothesis allows to sterically accommodate our ligand series.

For compound **9**, Induced Fit Docking (IFD)[46] produced a hypothesis consistent with SAR (Figure 8). The Boc tertiary-butyl group is possibly located next to Leu388 (helix 7). The exocyclic ligand amide oxygen possibly interacts with Arg190 (helix 2) critical for GLP-1 binding affinity.[44,47,48] The difluoro-cyclohexyl-group might be located in a hydrophobic pocket at the bottom near Tyr241 (helix 3). The piperazinone amide might interact with Gln234 (helix 3) and Met233 (helix 3), an important residue for peptide binding.**Error! Bookmark not defined.**,**Error! Bookmark not defined.** The indole is possibly located in the upper pocket area close to Trp306 (helix 5) and Arg380 (helix7). The postulated binding modes for compounds **9**, **14** and **19** are similar with the carboxylic acid in compound **19** possibly contacting the Lys197 (helix 2) side chain.

This model agrees to the GLP-1R active conformation with the indole oriented towards the outward-shifted helix 6. It is also consistent with the Cryo-Electron Microscopy (Cryo-EM) structure of activated GLP-1R with GLP-1 and G_s (5VAI, 4.1Å).[49] Removing the first residues of GLP-1 (His7-Ala8) in the Cryo-EM structure would allow accommodating the ligands.

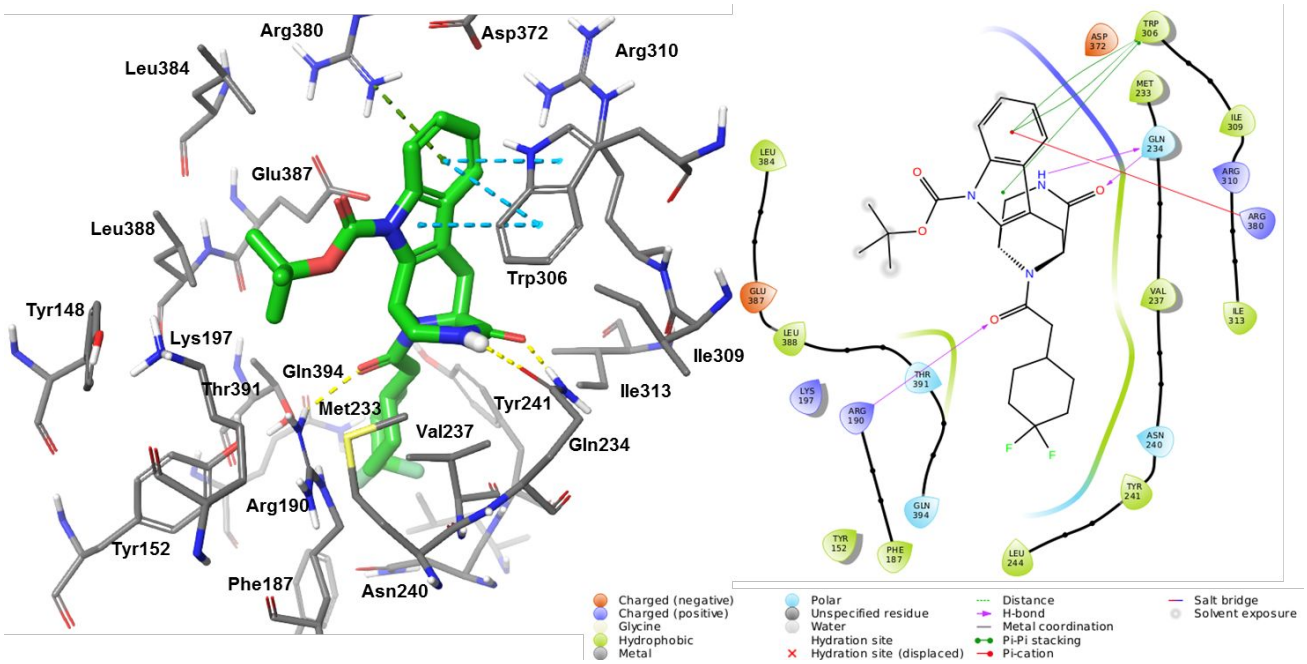

Figure 8. Postulated binding model for **9** (green carbon atoms) from Induced Fit Docking into the GLP-1R X-ray structure from 5NX2 (resolution 3.7 Å). Potential hydrogen bonds are indicated by dotted yellow lines, π–π interactions as dotted cyan lines and cation-π interactions as dotted green lines.

In-vitro ADME and *in-vivo* pharmacokinetic profiling of compound 19

Based on encouraging *in-vitro* pharmacological data of compound **19** in primary tissue, we evaluated its ADME profile to assess its potential for *in-vivo* studies as tool compound towards a proof-of-concept (PoC). Relevant *in-vitro* data for this compound are summarized in Table 2. Compound **19** is metabolically stable in human and mouse liver microsomes and exhibits high cell permeability in Caco-2 TC7 cell transwell experiments (P_{app} 32 * 10^{-7} cm/sec with a threshold of 20 * 10^{-7} cm/sec for highly permeable compounds) under standard test conditions conditions (pH 6.5 and 0.5% BSA apical and pH 7.4 and 5% BSA basolateral). Furthermore, this compound did not inhibit CYP3A4, displays good aqueous

solubility and is chemically stable under different conditions including GSH and mouse plasma. In mouse hepatocytes, compound **19** displays an intermediary clearance (0.145 mL/h/10^6 cells), which corresponds to 20% of hepatic blood flow.

Table 2. *In-vitro* and *in-vivo* profiling data for compound **19**.

Physicochemical data	**Value**	**Unit**
MW	585.64	Da
logD (pH 7.4, 25°C)	1.7	
clogP	4.5	
Solubility (pH 7.4)	>853	µM
Chemical stability (pH 1.1)	98	%
Chemical stability (pH 7.4)	99	%
Chemical stability (GSH)	100	%

***In-vitro* ADME data**	**Value**	**Unit**
Metabolic lability in microsomes (human)	20	%
Metabolic lability in microsomes (mouse)	5	%
CYP3A4 inhib. (IC_{50}, Substrate Midazolam)	>50	µM
CYP3A4 inhib. (IC_{50}, Substrate Testosteron)	>50	µM
Caco-2 P_{app}	32	10-7 cm/s
hERG inhibition (IC_{50}, Patch clamp)	>30	µM
Hepatic clearance (human)	0.184	mL/h/10e+06 cells
Hepatic clearance (mouse)	0.145	mL/h/10e+06 cells
Plasma stability (mouse)	98	%

***In-vivo* Pharmacokinetic data.**				
Treatment:	**Mouse**	**Rat**	**Rat +**	**Unit**
3 mg/kg i.v. / 10 mg/kg p.o.			**Rifampicin**	
C_{max} (p.o.)	227	106	1130	ng/mL
F (Bioavailability)	7.2	9.0	100	%
AUC_{last} (p.o.)	109	110	7340	h*ng/mL
V_{diss} (i.v.)	0.934	2.29	0.815	L/kg
Clearance (i.v.)	6.52	7.06	1.15	L/h/kg

However, after oral administration, the obtained mouse *in-vivo* pharmacokinetic (PK) data revealed extensive clearance (6.52 L/h/kg) with associated low oral bioavailability (F = 7.2 %) and a moderate volume of distribution (V_{diss}). Relevant data for mouse and rat PK studies after oral and i.v. administration are also summarized in table 4. The half-life in mouse plasma was low (0.29 h) and high concentrations of metabolically unchanged compound **19** were recovered in bile (rat fistula study, 74% of i.v. dose recovered in bile), suggesting that biliary excretion plays an important role in the clearance process for this compound.

In order to understand the mechanism for biliary clearance of this compound, we performed transporter studies employing HEK293 cells overexpressing the human organic anion transporters hOATP1B1 (organic anion transporting polypeptide 1B1, SLCO1B1) and hOATP1B3 (organic anion transporting polypeptide 1B3, SLCO1B3).[50] In particular OATP1B1 is one of the most highly expressed uptake transporters in human liver, and there are numerous reports regarding OATP1B1-mediated clinical drug-drug interactions.[51] The structure of **19**, containing an alkyl carboxylic acid moiety and relatively high molecular

weight, suggested that this compound could potentially be a substrate for these liver transporters.[52,53] Therefore we applied our internal *in-silico* transporter profile, a collection of 2D-QSAR models built from internal compounds and data, to this structure.[54] As expected, compound **19** was predicted to interact with OATP1B1 and OATP1B2 plus also classified as substrate for P-gp.

Subsequently compound **19** was experimentally identified as a substrate of hOATP1B1 and hOATP1B3 hepatic uptake transporter by a time-dependent increase of uptake in the overexpressing cell lines compared to the control HEK293 wild type cells (background) and with uptake ratios ranging from 6 to 22-fold, as obvious from inspection of Figure 9.

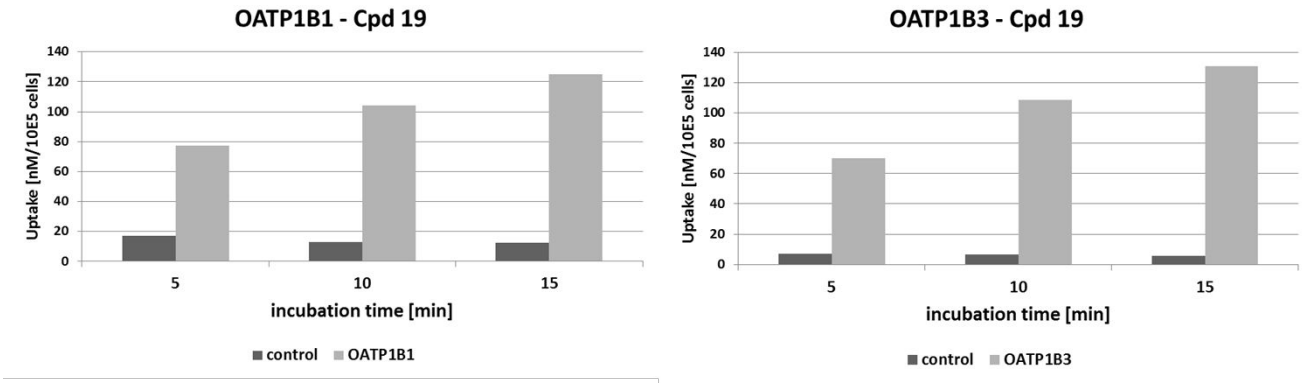

Figure 9. Compound **19** was identified as substrate of hOATP1B1 and hOATP1B3 transporter by a time-dependent incubation of 1 µM compound **19** with HEK cells overexpressing hOATP1B1 (left) and hOATP1B3 (right) or HEK293 wild type cells (control).

Additionally, we examined the efflux behavior of compound **19** in the presence and absence of efflux transporter inhibitors. Studies with Caco-2 TC7 cells revealed that, under isocratic

conditions (pH 7.4 and 0.5% BSA in apical and basolateral compartment), compound **19** shows a much lower permeability (0.18 * 10-7 cm/sec) and a high efflux ratio (ER = 247).

In presence of the efflux-transport-inhibitor cyclosporine A, the efflux could be inhibited (ER = 2). This finding shows that compound **19** is indeed a substrate for efflux transporters, most likely P-glycoprotein (P-gp) or MRP2 (multidrug resistance protein 1, MDR1, multidrug resistance-associated protein 2, ABCC2),[55,56] two important proteins in the cell membrane acting as ATP-dependent efflux pump with broad substrate specificity. Additionally, this result highly suggests an involvement of P-gp and MRP2 for active elimination of compound **19** in hepatocytes, as both transporters are expressed in the canalicular membrane.[57]

Although we could then identify the structural motif leading to a lowering of liver transporter recognition, the resulting compounds significantly lost their GLP-1R PAM activity (data not shown). Since a direct use of compound **19** for *in-vivo* proof-of-concept studies was precluded due to its poor pharmacokinetic profile, we then envisioned a study design which would still allow the evaluation of this compound *in-vivo*. Since the exposure of compound **19** was restricted by interactions with transporters in the small intestine, but especially in the liver, we hypothesized that its co-administration with the known OATP/MRP2 inhibitor Rifampicin would have a beneficial effect on plasma exposure of compound **19**.[58,59,60,61] Indeed, the mean exposure of compound **19** could be increased by a factor of 6 after i.v. and a factor of 85 after p.o. administration, when dosed to rat which had been pretreated with Rifampicin. This observation clearly supports our hypothesis that the above-mentioned transporters are responsible for restricted absorption and high hepatic clearance of compound **19**. Under these modified conditions, the plasma exposure of compound **19** was found sufficient to allow for an *in-vivo* proof-of-concept study (Table 4).

The rat PK study in presence and absence of Rifampicin was performed to confirm our *in-vitro* data from overexpressing cell lines, showing that the clearance of compound **19** is mainly driven by transporters especially of the OATP family in rodents. As this was clearly proven in a rat model, we selected an equal dose of 60 mg/kg p.o. in the pharmacological mice species. Moreover, the PK of Rifampicin in mice is described in the literature.[62] Here even at a lower dose of 10 mg/kg, C_{max} is reached after 1.5 h with a total concentration of 13 µM. This value is well above the IC_{50} values described for OATPs. The higher dose was used in our study to inhibit the efflux transporters in the intestine in parallel, which cannot easily be predicted, as the intestinal concentration is not known.

***In-vivo* pharmacology for compound 19**

As described above, compound **19** was applied in the presence of Rifampicin for a proof-of-concept study in ob/ob mice, which is a well-accepted disease model for T2DM (Figure 10).[63] Rifampicin was orally dosed 2.5 hours prior to the oral glucose-tolerance test (oGTT) to establish appropriate blood plasma concentration (data not shown). Subsequently, one hour prior to the oGTT, compound **19** was orally administered and, when indicated, GLP1(9-36)NH_2 was intraperitoneally co-administered 15 minutes prior to the oGTT. For the oGTT, mice were fasted overnight and 2 g/kg glucose challenge was used.

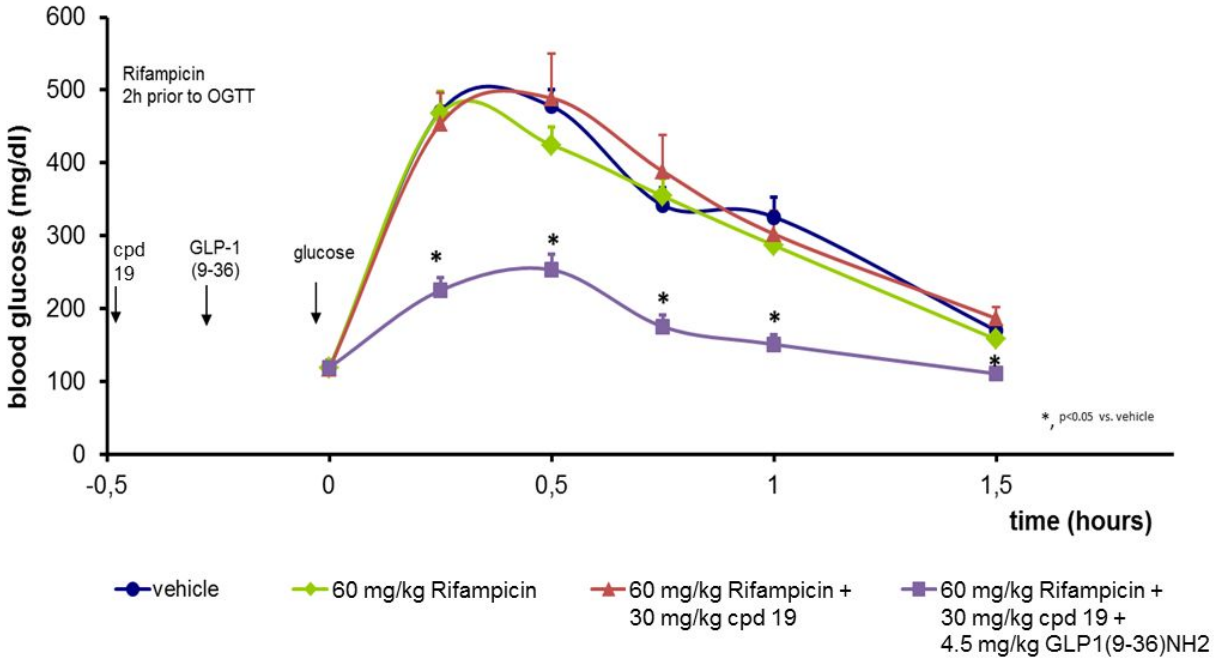

Figure 10. Proof-of-concept study for compound **19** in 11 weeks old ob/ob mice (n=7), an animal model of T2DM. Compound **19** required the presence of Rifampicin and GLP1(9-36)NH_2. GLP1(9-36)NH_2 was given intraperitoneally. In the presence of both GLP1(9-36)NH_2 and compound **19**, a significant reduction in blood glucose concentration was observed.

In all models used, compound **19** alone did not show any effect on blood glucose concentration in the absence of Rifampicin and/or GLP1(9-36)NH_2. Rifampicin at 60 mg/kg alone or in combination with compound **19** at 30 mg/kg orally dosed to ob/ob mice (n=7) had no effect on the blood glucose concentration in the oGTT. However, the intraperitoneal administration of GLP1(9-36)NH_2 to the combination of Rifampicin and compound **19** evoked a significant reduction in blood glucose concentration, as shown in Figure 11. In contrast, the peptide GLP1(9-36)NH_2 alone at a concentration of 4.5 mg/kg had no effect with or without addition of Rifampicin on blood glucose concentration (see Supporting Information). Furthermore, a dose-response relationship for the peptide GLP1(9-36)NH_2 and

compound **19** was established in normoglycemic C57Bl/6 mice (Figure 11). At all doses tested for the peptide GLP1(9-36)NH_2, compound **19** evoked a significant dose-dependent reduction of the blood glucose concentration during the oGTT.

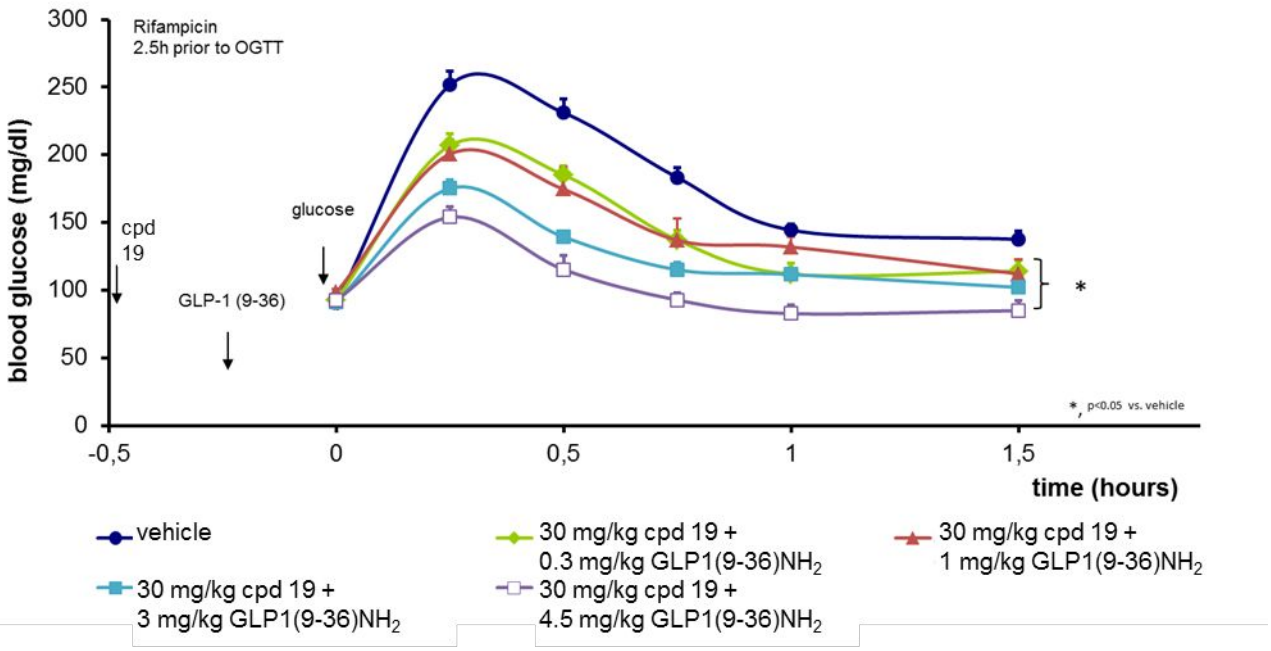

Figure 11. Dose-response relationship for compound **19** and the less active peptide GLP1(9-36)NH_2 in 11 weeks old normoglycemic C57Bl/6 mice (n=6). Compound **19** required the presence of Rifampicin and GLP1(9-36)NH_2 for a biological effect. GLP1(9-36)NH_2 has been given intraperitoneally at 0.3, 1, 3, and 4.5 mg/kg. Compound **19** evoked at all inactive GLP-1 doses a significant reduction in blood glucose concentration.

To finally demonstrate that the *in-vivo* effects of compound **19** strongly depend on the GLP-1 receptor, an oGTT in the GLP-1R$^{-/-}$ mouse was performed, as shown in figure 12. To explore the effect of compound **19** in GLP-1R$^{-/-}$ mice, the compound was tested in the presence of Rifampicin at 60 mg/kg and in the absence or in combination of intraperitoneally applied

GLP1(9-36)NH_2 (4.5 mg/kg). Rifampicin and compound **19** were both applied orally in this setting.

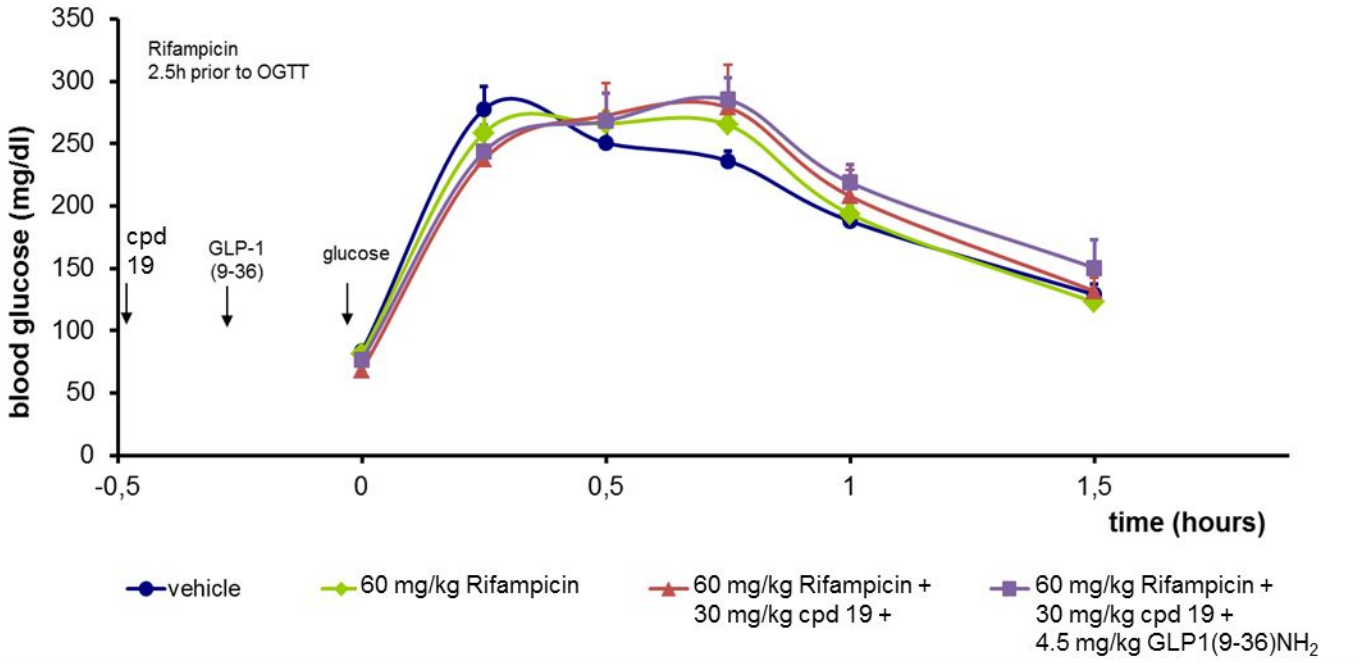

Figure 12. Demonstration of the GLP-1R dependent effect of compound **19** in 10 weeks old GLP-1$R^{-/-}$ mice (n=6). Compound **19** does not induce a significant blood glucose reduction in GLP1$R^{-/-}$ mice in the presence of Rifampicin and GLP1(9-36)NH_2 at the highest dose tested.

Under all the conditions tested in GLP-1$R^{-/-}$ mice, compound **19** did not show any effect on blood glucose concentration, strongly supporting our hypothesis that the interesting pharmacological effect of this positive allosteric modulator **19** is directly mediated by its interaction with the GLP-1 receptor (Figure 12).

Conclusion

The glucagon-like peptide 1 (GLP-1) hormone is secreted from intestinal L-cells after food intake and plays a crucial role for blood glucose regulation and control of appetite and body weight. Its activation of GLP-1R triggers glucose-dependent insulin secretion and leads to suppression of glucagon secretion in the pancreas. For treatment of T2DM, several approaches, like GLP-1 mimetics and DPP-IV inhibitors, are directed to enhance activation of GLP-1R. In this contribution we report a new compound as positive allosteric modulator (PAM) for this important GPCR, namely compound **19** as potent, non-covalent and selective PAM based on a 3,4,5,6-tetrahydro-1H-1,5-epiminoazocino[4,5-b]indole scaffold. This PAM is able to turn the significantly less active metabolite GLP1(9-36)NH_2 into a potent ligand able activate GLP-1R in a similar manner as the active GLP-1 peptide itself does.

Our best compound **19** demonstrates high activity and selectivity in various functional assays. Due to its favorable *in-vitro* ADME and *ex-vivo* profile, it was further evaluated *in-vivo*. We could explain the observed high biliary clearance in animal PK studies and attributed this to interaction of compound **19** with human organic anion transporters hOATP1B1 and hOATP1B3. This finding required co-administration of the transporter inhibitor Rifampicin for a successful *in-vivo* proof-of-concept study of compound **19** as tool for our proposed mode of action.

Unfortunately, the need of exogenous addition of GLP1(9-36)NH_2 to elicit a significant response on glucose homeostasis experiments *in-vivo* clearly shows that the PAM ability of our best compound **19** is not yet sufficient to induce a significant response under physiological conditions without addition of this exogenous peptide. The requirement of exogenous GLP1(9-36)NH_2 for a successful *in-vivo* effect might not be so surprising, since the EC_{50}-shift observed for GLP1(9-36)NH_2 in the presence of 10 μM of our best PAM **19** in

pancreatic 1.1B4 cells was not sufficient to match the EC_{50} value of GLP1(7-36)NH_2. GLP1(7-36)NH_2 is approximately 10,000 more potent than its less active counterpart GLP1(9-36)NH_2. Taking into account the higher concentration of the less active metabolite in vivo, a potentiation by a factor of ~2,500 is anticipated to be required at an *in-vivo* relevant compound concentration to achieve full therapeutic utility.

Therefore even if compound **19** has proven to be a valuable tool to proof the feasibility of GLP1(9-36)NH_2 potentiation *in-vivo*, the validity of this approach under physiological conditions remains an open question. The data presented herein suggest that a significant amount of optimization would still be needed to arrive at a successful clinical candidate. In our opinion, it is questionable, whether the challenging goal of identifying a non-covalent, orally available GLP1(9-36)NH_2 potentiator that works under physiological conditions can be reached at all.

Experimental section

Biological Assays.

Min6 Ca^{2+} mobilization assay. MIN6-c4 cells (Osaka University)[64] were plated at a density of $5x10^4$ cells per well into black 96-well plates and cultured for 20-24 h at 37 °C and 5% CO_2. For cell loading, culture supernatants were aspirated and 100 µL assay buffer (Krebs-Ringer buffer, 10 mM HEPES, 0.1% BSA, 2.5 mM glucose) and an equal volume of Calcium 6 dye (FLIPR® Calcium 6 Assay Kit, Molecular Devices, R8191) dissolved in the same buffer according to instructions of the manufacturer were added to each well. Cells were incubated for 70 min at 37 °C / 5% CO_2 and equilibrated for additional 10 min at room temperature in the dark. To assess the effect of test compounds on glucose-mediated increase in intracellular Ca^{2+}, a volume of 50 µL assay buffer containing 75 mM glucose (resulting in

a final concentration of 15 mM glucose) and test compounds or DMSO was added per well during detection on a FLIPR® Tetra instrument (molecular devices). For low glucose controls, 50 µL starvation buffer without additional glucose was added to keep the final glucose concentration at 2.5 mM. Calcium flux was quantified by calculating the area under the curve of fluorescence readings from 3 sec. to 372 sec.

cAMP stimulation assay in PSC-HEK293 cell line stably expressing human GLP-1R. *In-vitro* cellular assays for GLP-1R agonists and positive allosteric modulators were conducted in 1536-well plates using thaw-and-use frozen cells. Prior to use, frozen cells were thawed quickly at 37 °C and washed (5 min at 900 rpm) with 20 mL cell buffer (1x HBSS; 20 mM HEPES, 0.1% BSA). Cells were re-suspended in assay buffer (cell buffer plus 2 mM IBMX) and adjusted to a cell density of 1 million cells/mL. To a 1536-well microtiter plate, 2 µL cells are added (final 2000 cells/well) and 2 µL compound for an agonist assay. For a PAM assay, two assay formats were applied, namely (a) an enhancer assay with 1 µL of different doses of the compound and 1 µL of a fixed concentration (EC_{20}) of GLP1(9-36)NH_2, and (b) a shift assay with 1 µL of different doses of GLP1(9-36)NH_2 and 1 µL of 10 µM and 3 µM compound. The mixtures containing 2 µL of each cells and compounds were incubated for 30 min. at room temperature.

The cAMP content of cells was determined using a kit from Cisbio Corp. (cat. no. 62AM4PEC) based on HTRF (Homogenous Time Resolved Fluorescence). After addition of HTRF reagents diluted in lysis buffer (kit components), plates were incubated for 1 h, followed by measurement of the fluorescence ratio at 665 / 620 nm. Dose-response results were calculated with the internal software Biost@t-Speed v 2.0 HTS using a 4-parameter logistic model.

cAMP stimulation assay in the human pancreatic ß-cell line 1.1B4. *In-vitro* cellular assays of GLP-1(7-36)NH_2, GLP1(9-36)NH_2 and test compounds were conducted using the human pancreatic ß-cell line 1.1B4. Upon GLP-1R activation, the 1.1B4 cells accumulate intracellular cyclic adenosine monophosphate (cAMP). Cyclic AMP formation was measured using a commercial immunoassay technology with HTRF readout. In these experiments, all reagents necessary for quantification of cAMP were supplied in a kit (cat. no. 62AM4PEC from Cisbio Corp., France) and applied according to protocols supplied by the vendor. Two assay formats were applied, namely (a) an enhancer assay with a compound concentration-response curve and a fixed concentration of 10 nM GLP1(9-36)NH_2, and (b) a shift assay with a GLP1(9-36)NH_2 concentration-response curve, and a fixed concentration of 1 µM compound. 20,000 cells were seeded into a 96-well microtiter plate. Following overnight culturing, cells were washed twice and serial dilutions of GLP-1R ligand or test compound with or without the respective fixed concentration of either test compound or GLP1(9-36)NH_2 were transferred to the cells. After incubation for 30 min with the test agents, the cells were lysed and prepared for cAMP determination according to the manufacturer's description. Data points were obtained by fluorescence measurement at 665 and 620 nm, calculation of 665/620 nm ratio and expression in percentage of effect relative to negative (0%) and positive (100%) controls. The negative control was assay buffer (1x HBSS, 0.1% BSA, 1 mM IBMX) and the positive control was GLP-1(7-36)NH_2. Concentration-response results were calculated with internal software Biost@t-Speed v 2.0 LTS using a 4-parameter logistic model. The adjustment was obtained by non-linear regression using the Marquardt algorithm in SAS v9.1.3.

Rat pancreatic islet isolation and islet dispersion. For islet isolation, a collagenase enzyme solution was injected into the common bile duct of the euthanized male animal (Sprague Dawley, 225 g). The pancreas was excised and further digested at 37°C for 15 min. The

obtained tissue suspension was washed three times with cell culture medium 199 containing 10% newborn fetal calf serum, followed by repeated filtration through a 600 μm screen. In a further purification step, gradient separation of islets from pancreatic acinar tissue using Histopaque was applied. Finally, islets were handpicked under a dissecting microscope and cultured overnight in an incubator under 95% O_2/5% CO_2 at 37°C. To disperse islet cells into cell suspensions, islets were digested with Accutase solution, seeded into a 96-well cell culture dish and cultured for up to 4 days at 37°C in a humidified CO_2 incubator under 95% O_2/5% CO_2 prior to glucose-stimulated insulin secretion assays.

Functional activity in glucose-stimulated insulin secretion assay and insulin measurement. All determinations of insulin secretion were performed in dispersed pancreatic islets under static incubation. Briefly, dispersed islets seeded into 96-well plates were pre-incubated for 1 h at 37°C in Krebs–Ringer (KR) buffer containing 120 mM NaCl, 4 mM KCl, 2 mM $MgCl_2$ * $6H_2O$, 2 mM $CaCl_2$ * $2H_2O$, 1.19 mM NaH_2PO_4 * H_2O, 20 mM $NaHCO_3$, 10 mM HEPES equilibrated to pH 7.4, 0.05% bovine serum albumin, 5.6 mM glucose. The pre-incubation medium was then replaced with KR buffer supplemented with different glucose concentrations (basal: 3 mM; stimulatory: 15 mM) as well as other test agents. After incubation for 2 h at 37°C, the supernatant was collected and stored at -80°C for later analysis of insulin content. KR buffer supplemented with 1.25% triton X100 was added to the remaining cells for lysis. The cell lysate was stored as well at -80°C for later analysis of insulin content. Insulin was measured by ELISA (Cisbio Corp., France) using a Tecan Envision plate reader. Two measurements of fluorescence upon excitation at 320 nm are carried out at 620 nm for the cryptate emission and at 665 nm for the specific signal emitted by the acceptor. Results are calculated from the 665 nm / 620 nm ratio in percentage of insulin secreted relative to total insulin and expressed as n-fold insulin secretion versus respective controls.

ADME assays. Permeability assays were performed with Caco-2/TC7 cells.[65,66,67,68] Conditions for the apical compartment were pH 6.5; 0.5% bovine serum albumin (BSA); compound concentration 20 µM; basolateral compartment pH 7.4; 5% BSA; 2 hours incubation time. Efflux was determined under isocratic conditions with pH 7.4 and 0.5% BSA in both compartments and compound concentration of 2 µM. All analyses were performed with LC-MS/MS.

CYP inhibition assays [69] were performed with pooled and phenotyped human hepatic microsomes (0.1 mg/mL for CYP3A4). As cofactors, 6 mM $MgCl_2$, 0.5 mM EDTA, 1 mg/mL BSA, 1 mM NADPH were used; compound concentration tested was in the range of 0.001 – 200 µM (in duplicate). Results were expressed as % inhibition or IC_{50}. As substrates midazolam and testosterone were used for CYP3A4 [70,71,72,73,74,75,76,77,78,79,80.]

Lability assays were performed with pooled and phenotyped human liver microsomes taking samples at time 0 and time 20 minutes for LC-MS/MS analysis[69]. Clearance *in vitro* was determined using primary human hepatocytes at 1.4 * 10^{-6} cells/mL or mouse hepatocytes[69]. Individual compound concentration varied from 0.5 µM to 5 µM. CYP contribution was determined by addition of either quinidine for CYP2D6 inhibition or ketoconazole for CYP3A4 inhibition to the assay plate. All bioanalytical analyses were performed by LC-MS/MS.

Transporter assays with recombinant cell lines for OATP1B1 and OATP1B3. HEK^{TR}, HEK^{TR}-hOATP1B1 and HEK^{TR}-hOATP1B3 cell lines were seeded at 1 x 10^5 cells/well/100 µL onto poly-D-Lysine coated 96-well plates (BD BioCoat) in culture medium and experiments were conducted one day after cell seeding. All inhibition experiments were performed with HBSS assay buffer in 96-well plates in quadruplet at 37 °C. The buffer volume was 50 µL in each well. Overexpressing cells and control cells were always treated in

parallel. Cells were washed with 200 µL HBSS assay buffer (37°C) and then incubated in the presence of the substrate. Uptake was stopped by adding 150 µL/well ice-cold HBSS assay buffer. Solution was removed and cells were washed two times with 200 µL/well ice-cold HBSS assay buffer. After the complete removal of the washing solution cells were lysed and uptake was quantified by LSC or LC-MS/MS techniques. Functionality of the assay (not-shown) was proven with probe substrates for OATP1B1 and OATP1B3 (1 µM ^{3}H-E17βG (10 min.) and 0.5 µM ^{3}H-CCK8 (5 min.)) in the absence and the presence of the probe inhibitor Rifampicin (10 µM) for both transporters.

Animal studies. All studies in animals were conducted in accordance with German laws for protection of animals. Furthermore, the investigation conforms to the Guide for the Care and Use of Laboratory Animals published by the U.S. National Institutes of health.

Pharmacokinetic parameters in rats and mice. The plasma concentrations and pharmacokinetic parameters of compound **19** were determined after single intravenous administration of 3 mg/kg body weight in solution (75% purified water: 25% (75% Glycoferol: 25 % Cremophor)) and single oral administration of 10 mg/kg bodyweight in wet milled suspension (0.6% methylcellulose : 0.5% Tween 80 in purified water) to male Wistar rats (n = 3 per route) and to female C57Bl6 mice (n= 24 per route). Additionally Rifampicin (40 mg/kg bodyweight solved in 0.6% methylcellulose, 0.5% Tween 80 in purified water) was orally co-administered 2 h before i.v or p.o. dosing of compound **19**. Sampling time points were 0.083, 0.25, 0.5, 1, 2, 4, 6, 8 and 24 h after intravenous route and 0.25, 0.5, 1, 2, 4, 6, 8 and 24 h after oral route for both species. Analysis was performed with ESI-LC/MS–MS assay of compound **19** in heparinized plasma after protein precipitation with acetonitrile, with a limit of quantitation (LOQ) of 1 ng/mL in rat, and of 5 ng/mL in mice.[81] The

pharmacokinetic parameters were calculated by the program WinNonlin 6.4 using a non-compartmental model and linear trapezoidal interpolation calculation.

In-vivo pharmacology studies. Adult male ob/ob, C57Bl/6J and GLP-1R knockout (GLP-1R$^{-/-}$) mice were obtained from Charles River (Sulzfeld, Germany). Animals at 10–11 weeks of age were used. Mice were housed in environmentally controlled conditions with a 12 hour light/dark cycle and had free access to water and standard rodent pellet food. Prior to the test procedures blood glucose concentration (BG) of the ob/ob mice was determined to randomize the animals for the study. Animals were fasted overnight. On the day of the test, fasted animals were treated 2.5 h prior to the oGTT orally with Rifampicin at 60 mg/kg, 1 hour prior to the oGTT orally with compound **19** and 15 minutes prior to the oGTT intraperitoneally with inactive GLP1(9-36)NH2 (Bachem, Germany) at the doses indicated. The oGTT has been performed with an oral administration of glucose at 2 g/kg bodyweight. Blood glucose levels were determined in blood samples from the tail vein at 0 (prior to glucose administration), and 15, 30, 60 and 90 min after glucose administration using standard glucometers: Accu-chek (Roche) or Star Strip Xpress (DSI) where appropriate.

Computational methods. Calculations were performed using the Schrödinger molecular modeling suite.[82] Protein structures from the Protein Data Bank (PDB)[83] were prepared using the Protein Preparation Wizard.[84] Ligand structures were prepared with LigPrep and minimized using OPLS3.[85,86] Molecules were treated in ionized form at neutral pH. Hydrogen bond networks of X-ray structures were optimized using the Protein Preparation Wizard. Final models were minimized by a staged protocol in Prime using OPLS3.

Ligands were docked into the GLP-1R model and the X-ray structure from PDB file 5NX2 using Glide XP[Error! Bookmark not defined.] with weak core constraints to the indole towards a reasonable alignment. Final poses were optimized using Prime with side chains in a 3 Å

sphere around ligands flexible. Induced Fit Docking (IFD)[46] was applied for consistent poses of the reference ligand **9**. Subsequently for other ligands, the docked pose of the reference served for weak core constraints using the indole substructure of the tetracyclic core.

In silico ADME models were generated using data from multiple internal series.[54] Model building for endpoints like human microsomal lability and PXR activation is described elsewhere.[87,88] Pretreatment included removal of counterions and smaller fragments, neutralization plus canonization of structures. Canonical 3D geometries including hydrogen positions were generated using Corina.[89,90] The 2D-QSAR models were based on MOE,[91] CATS[92] and Ghose-Crippen atom type[93] descriptors (internal implementations for both latter sets). For quantitative models the program Cubist[94,95] constructing a rule-based decision tree as consensus of five individual trees is applied, while classification models are developed using the program C5.0.[96] A GA-based approach[87,88] for variable selection maximizes the sum of regression coefficients or minimizes classification errors for training and test sets.

For OATP1B1 interaction, a model was obtained with a crossvalidated r^2 value of 0.436 and an r^2 value of 0.757. Prediction using a test set of 258 compounds resulted in an r^2 value of 0.593. For OATP1B3, a model was obtained with a crossvalidated r^2 value of 0.423 and an r^2 value of 0.828, while prediction using 259 compounds led to an r^2 value of 0.548. Both models can be applied qualitatively only. For classification of P-gp substrates, an internal C5 decision tree classification based on a dataset from Wang et al. [97] was derived. This classifier is based on a training set of 249 and a test set of 82 compounds with prediction quality of > 96 % for both sets.

Chemistry. Solvents and other reagents were used as received without further purification. Normal phase column chromatography was carried out on Merck silica gel 60 (230–400 mesh). Reversed phase high pressure chromatography was conducted on an Agilent 1100

instrument using an Agilent Prep C18 column (10 μm, 30 mm × 250 mm). Varying ratios of acetonitrile and 0.1% trifluoroacetic acid in water were used as solvent systems. Thin-layer chromatography was carried out on TLC aluminum sheets with silica gel 60F254 from Merck. NMR spectra were recorded in $CDCl_3$ or DMSO-d_6 on either a Bruker ARX 500 or a Bruker DRX 400. Chemical shifts are reported as δ values from an internal tetramethylsilane standard. Purity and characterization of compounds were established by a combination of analytical UPLC–MS and NMR analytical techniques. All tested compounds were found to be >95% pure by analytical UPLC–MS analysis unless otherwise stated. UPLC–MS analyses were performed with a Waters ACQUITY UPLC system, column C18 1.7 μm, 2.1 mm × 50 mm; gradient (H_2O + 0.05% TFA)/(MeCN + 0.035% TFA) 95:5 (0 min) to 5:95 (2 min) to 5:95 (2.6 min) to 95:5 (2.7 min) to 95:5 (3 min), flow rate 0.9 mL/min, temperature 55 °C; mass detector Waters SQD single quadrupole, ESI+ mode.

Synthetic Procedures. Synthetic procedures are illustrated by the synthesis of compound **19**. For synthesis of other compounds please see Supporting Information.

tert-butyl 3-((S)-2-((((9H-fluoren-9-yl)methoxy)carbonyl)amino)-3-((2S,4R)-2-(hydroxymethyl)-4-(2-methoxy-2-oxoethyl)pyrrolidin-1-yl)-3-oxopropyl)-1H-indole-1-carboxylate (16)

A mixture of **9b** (5.0 g, 9.5 mmol), methyl 2-((3R,5S)-5-(hydroxymethyl)pyrrolidin-3-yl)acetate **15** (1.73 g, 9.97 mmol), HATU (4.33 g, 11.39 mmol) and DIPEA (3.3 mL, 18.9 mmol) in THF (30 mL) was stirred at rt overnight. The reaction mixture was evaporated and purified by column chromatography on silica gel (eluent Hexanes:EtOAc 1:1 to 100 % EtOAc) to give the desired product **16** as a white foam (2.45 g, 37%).^{1}H NMR (400 MHz, DMSO-d6) δ 7.94-8.07 (m, 1H), 7.70-7.90 (m, 2H), 7.48-7.74 (m, 4H), 7.17-7.44 (m, 4H), 4.64-4.75 (m, 1H), 4.38-4.59 (m, 1H), 4.12-4.26 (m, 1H), 3.45-3.61 (m, 1H), 3.57 (s, 3H),

3.15-3.29 (m, 1H), 2.91-3.14 (m, 1H), 2.80 (br t, *J* =9.11 Hz, 1H), 2.22-2.43 (m, 1H), 2.07-2.22 (m, 1H), 1.74 (br s, 1H), 1.50-1.63 (m, 1H), 1.35-1.47 (m, 1H), 0.83-0.89 (m, 9H), 0.66-0.74 (m, 1H). LCMS: 1.56 min, m/z 586.2 [M+H]+.

14-((9H-fluoren-9-yl)methyl) 12-(tert-butyl) (2R,6S,13S,13aS)-2-(2-methoxy-2-oxoethyl)-5-oxo-1,2,3,5,6,7,13,13a-octahydro-12H-6,13-epiminopyrrolo[1',2':1,2]azocino[4,5-b]indole-12,14-dicarboxylate (**17**)

To a solution of **16** (2.45 g, 3.59 mmol) in CH_2Cl_2 (60 mL), Dess-Martin periodinane was added (3.0 g, 7.2 mmol) and the mixture stirred at RT overnight. Then the mixture was quenched with saturated $NaHCO_3$ and then with $NaHSO_3$. The organic layer was dried over $MgSO_4$, filtered and evaporated. The residue was taken up in HCO_2H (45 mL) and stirred at rt for 1 h. LC/MS analysis showed a 1:1 mixture of desired product **17** and Boc-deprotected derivative. The mixture was diluted with CH_2Cl_2 and H_2O and extracted. The water phase was then extracted once more with CH_2Cl_2 and purified by column chromatography using EtOAc: Heptane: MeOH gradient to give the desired product as a white solid (939 mg, 40%).^{1}H NMR (400 MHz, DMSO-d_6) ^{1}H NMR (400.23 MHz, DMSO-d6) δ ppm 8.02 (br t, *J* = 8.56, 8.56 Hz, 1 H),7.91 (br d, *J* = 7.70 Hz, 1 H), 7.76 (br dd, *J* = 18.65, 7.40 Hz, 1 H), 7.65 (br d, *J* = 7.82 Hz, 1 H), 7.56 (m, 3 H), 7.40 (m, 5 H), 7.24 (m, 4 H), 6.17 (m, 1H isomer 1), 6.10 (m, 1H, isomer 2), 4.71 (br s, 1 H), 4.58 (m, 3 H), 4.31 (m, 2 H), 4.23 (br d, *J* = 5.13 Hz, 1H), 4.04 (ddd, *J* = 14.12, 6.97, 6.79 Hz, 1 H), 3.88 (br d, *J* = 11.49 Hz, 1 H),3.60 (m, 1 H), 3.53 (br d, *J* = 12.84 Hz, 4 H), 3.43 (u), 2.94 (br s, 1 H), 2.75(m, 2 H), 2.50 (u), 2.38 (m, 3 H), 2.26 (m, 2 H), 2.17 (m 2H), 1.56 (m, 1H), 0.52 (m, 1H). LCMS: 2.08 min, m/z 662.28 [M+H]+.

tert-butyl (2R,6S,13S,13aS)-2-(2-methoxy-2-oxoethyl)-5-oxo-1,2,3,5,6,7,13,13a-octahydro-12H-6,13-epiminopyrrolo[1',2':1,2]azocino[4,5-b]indole-12-carboxylate (18)

A solution of **17** (670 mg, 1.10 mmol) in a mixture of THF: dimethyl amine (2:1, 30 mL) was stirred at rt overnight. The solvent was evaporated, and the residue purified by column chromatography on silica gel (gradient EtOAc: MeOH 100:0 to 4:1) to give the desired product singel diastereomer **18** as a white solid (323 mg, 72%). ^{1}H NMR (600 MHz, $CDCl_3$-d) δ 8.10 (d, *J* = 8.53 Hz, conformer 1, 1H), 8.01 (d, *J* = 8.34 Hz, conformer 2, 1H), 7.46-7.48 (m, 1H), 7.25-7.39 (m, 2H), 7.00 (d, *J* = 4.58 Hz, conformer 1, 1H), 6.36 (d, *J* = 4.20 Hz, conformer 2, 1H), 5.54 (br d, *J* = 2.82 Hz, conformer 2, 1H), 4.83 (br d, *J* = 5.96 Hz, conformer 1, 1H), 4.23 (m, conformer 2, 1H), 4.17 (m, conformer 1, 1H), 3.68 (m, 1H), 3.65 (s, 3H), 3.31 (d, *J* = 16.44 Hz, conformer 1, 1H), 2.99-3.20 (m, 3H), 2.60 (m, 1H), 2.48 (m, 1H), 2.40-2.20 (m, 4H), 2.07-1.92 (m, 3H), 1.72-1.83 (m, 2H), 1.73 (s, 9H), 1.32 (m, 2H), 0.97 (m, 1H). LC-MS Method A: 1.44 min, m/z 440.21 [M+H]+. The relative configuration was unambiguously determined by 2D NMR. See supporting information for details.

2-((2R,6S,13S,13aS)-12-(tert-butoxycarbonyl)-14-(2-(4,4-difluorocyclohexyl)acetyl)-5-oxo-2,3,5,6,7,12,13,13a-octahydro-1H-6,13-epiminopyrrolo[1',2':1,2]azocino[4,5-b]indol-2-yl)acetic acid (19)

Step 1: A mixture of 2-(4,4-difluorocyclohexyl)acetic acid (34 mg, 0.189 mmol), **18** (50 mg, 0.09 mmol), HATU (42 mg, 0.11 mmol) and DIPEA (47 µL, 0.27 mmol) in THF (4 mL) was stirred at rt overnight. The mixture was diluted with dichloromethane and washed with saturated $NaHCO_3$. The organic layer was washed with 10% aq. citric acid, dried and evaporated, and used in the next step without further purification.

Step 2: To a solution of the above crude (64 mg, 85.4 mmol) in THF:H_2O 1:1 (8 mL) at 0°C, LiOH (21mg, 854 mmol) was added. The mixture was stirred for 20 min at 0°C and then carefully taken to pH 6 with slow addition of citric acid (10% solution in water). The mixture was then extracted with dichloromethane and the organic layer washed with water. The water

layer, which still contained some product, was extracted with EtOAc (3 times) and the organic layers were dried over $MgSO_4$, filtered and evaporated. The residue was dissolved in DMF and purified by HPLC to give the desired product **19** as a white solid (17 mg, 38%). ^{1}H NMR (600 MHz, $CDCl_3$-d) δ 8.07 (d, *J* = 8.53 Hz, conformer 1, 1H), 7.99 (d, *J* = 8.34 Hz, conformer 2, 1H), 7.39-7.48 (m, 1H), 7.27-7.37 (m, 2H), 7.00 (d, *J* = 4.58 Hz, conformer 1, 1H), 6.34 (d, *J* = 4.20 Hz, conformer 2, 1H), 5.55 (br d, *J* = 2.82 Hz, conformer 2, 1H), 4.91 (br d, *J* = 5.96 Hz, conformer 1, 1H), 4.22 (m, conformer 2, 1H), 4.17 (m, conformer 1, 1H), 3.72 (m, 1H), 3.28 (d, *J* = 16.44 Hz, conformer 1, 1H), 2.94-3.19 (m, 2H), 2.59 (m, 1H), 2.48 (m, 1H), 2.38-2.20 (m, 4H), 1.91-2.12 (m, 3H), 1.72-1.83 (m, 2H), 1.70 (s, 9H), 1.29 (m, 2H), 0.97 (m, 1H). LCMS Method A: RT 1.82 min, m/z 586.2 [M+H]+; HRMS m/z Calculated for $C_{31}H_{37}F_2N_3O_6$: 585.2650. found: 585.2652. Chiral HPLC Method A; 6.89 minutues.

Author information

Corresponding Authors

*M.M.: phone, ++49-69-305-44713; e-mail, Maria.MendezPerez@sanofi.com

*H.M.: phone, ++49-69-305-84329; e-mail, Hans.Matter@sanofi.com

Acknowledgements

We would like to thank our colleagues O. Eckhardt, I. Burmann, A. Sihorsch and A. Struppmann for synthesis and U. Messinger, T. Klöckener and S. Stengelin for technical support. We also gratefully acknowledge interesting discussions with W. Czechtizky, M. Dreyer, A. Evers, G. Hessler, A.A. Konkar, A. Plowright, and P. Larsen.

Abbreviations

ADME, Absorption, distribution, excretion, metabolism; Boc, Butyloxycarbonyl; BSA, Bovine serum albumin; cAMP, Cyclic adenosine monophosphate; CRF1-R, Corticotropin-releasing hormone receptor 1; CYP3A4, Cytochrome P450 3A4; DIPEA, N,N-Diisopropylethylamine; DMAP, 4-Dimethylaminopyridine; DMEM, Eagle's minimal essential medium; DMF, Dimethylformamide; DMSO, Dimethylsulfoxide; ECD, Extracellular domain; EDC, 1-Ethyl-3-(3-dimethylaminopropyl)carbodiimide; ER, Efflux ratio; Fmoc, Fluorenylmethyloxycarbonyl; GIP, gastric inhibitory polypeptide; GIPR, gastric inhibitory polypeptide receptor; GCGR, Glucagon receptor; GLP-1, Glucagon-like peptide 1 ; GLP-1R, Glucagon-like peptide 1-receptor; GPCR, G protein-coupled receptor; GSH, Glutathione; GSIS, Glucose-stimulated insulin secretion; HATU, 1-[Bis(dimethylamino)methylene]-1H-1,2,3-triazolo[4,5-b]pyridinium 3-oxid hexafluorophosphate; HBSS, Hank's balanced salt solution; HEK293, Human embryonic kidney cells 293; HEPES, 4-(2-hydroxyethyl)-1-piperazineethanesulfonic acid; HPLC, High-performance liquid chromatography; HTRF, Homogeneous time-resolved fluorescence; HTS, High-throughput screening; hOATP1B1, Human organic anion transporting polypeptide 1B1; hOATP1B3, Human organic anion transporting polypeptide 1B3; IFD, Induced fit docking; KR, Krebs-Ringer; MD, Molecular dynamics; MeMgBr, Methylmagnesiumbromide; MRP2, Multidrug resistance-associated protein 2; MW, Molecular weight; OATP, Organic anion transporting polypeptide; OATP1B1, Organic anion transporting polypeptide 1B1; OATP1B3, Organic anion transporting polypeptide 1B3; oGTT, oral glucose-tolerance test; PAM, Positive allosteric modulator; P-gp, P-glycoprotein; PK, Pharmacokinetic; PoC, Proof-of-concept; QSAR, Quantitative structure-activity relationship; rt., Room temperature; SAR, Structure-activity relationship; T2DM, Type 2 diabetes mellitus; THF, Tetrahydrofuran; TM, Transmembrane domain; VIPR2, vasoactive intestinal peptide 2 receptor; V_{diss}, Volume of distribution; Z, Benzyloxycarbonyl; 7TM, 7-Transmembrane-helix domain.

Supporting Information

Supporting Information is available free of charge on the ACS Publications website at DOI: 10.1021/acs.jmedchem.xxx.

Chemistry methods and general procedures. Synthesis schemes and procedures for compounds **9** and **14**. Structure elucidation of compound **18**. Results for selectivity testing for compounds **9**, **14** and **19**. Pharmacokinetic data for compound **19**. In vitro data for literature reference compounds and / or close analogues. Effect of i.p. administration of GLP1(9-36)NH_2 (9 mg/kg) on glucose excursion in C57BL/6 mice. In-vivo effect of GLP1(9-36)NH_2 of compound 9 and BETP in combination with GLP1(9-36)NH_2 (PDF).

Binding hypothesis of compound **19** in complex with GLP1-R (PDB).

Molecular formula strings of all compounds (CSV).

References

1 De Graaf, C.; Donnelly, D.; Wootten, D.; Lau, J.; Sexton, P.M.; Miller, L.; Ahn, J.-M-; Liao, J.; Fletcher, M.M.; Yang, D.; Brown, A.J.H.; Zhou, C.; Deng, J.; Wang, M.-W. Glucagon-Like Peptide-1 and Its Class B G Protein-Coupled Receptors: A Long March to Therapeutic Successes. *Pharmacol. Rev.* **2016**, *68*, 954-1013.

2 Lorenz, M.; Evers, A.; Wagner, M. Recent Progress and Future Options in the Development of GLP-1 Receptor Agonists for the Treatment of Diabesity. *Bioorg. Med. Chem. Lett.* **2013**, *23*, 4011-4018.

3 Turton, M.D.; O'Shea, D.; Gunn, I.; Beak, S.A.; Edwards, C.M.; Meeran, K.; Choi, S.J.; Taylor, G.M.; Heath, M.M.; Lambert, P.D.; Wilding, J.P.; Smith, D.M.; Ghatei, M.A.; Herbert, J.; Bloom, S.R. A Role for Glucagon-like Peptide-1 in the Central Regulation of Feeding. *Nature* **1996**, *379*, 69-72.

4 Prasad-Reddy, L.; Isaacs, D. A Clinical Review of GLP-1 Receptor Agonists: Efficacy and Safety in Diabetes and Beyond. *Drugs Context* **2015**, *4*, 212283.

5 Manandhar, B.; Ahn, J.-M. Glucagon-like Peptide-1 (GLP-1) Analogs: Recent Advances, New Possibilities, and Therapeutic Implications. *J. Med. Chem.* **2015**, *58*, 1020-1037.

6 Irvin, N.; Flatt, P.R. New Perspectives on Exploitation of Incretin Peptides for the Treatment of Diabetes and Related Disorders. *World J. Diabetes* **2015**, *10*, 1285-1295.

7 Edmonds, D. J.; Price, D. A. Oral GLP-1 Modulators for the Treatment of Diabetes. *Ann. Rep. Med. Chem.* **2013**, *48*, 119-130.

8 Willard, F.S.; Bueno, A.B.; Sloop, K.W. Small Molecule Discovery at the Glucagon-like Peptide Receptor. *Exp. Diabetes Research* **2012**, Article ID 709893, 1-9.

9 Lau, J.; Bloch, P.; Schaffer, L.; Pettersson, I.; Spetzler, J.; Kofoed, J.; Madsen, K.; Knudsen, L.B..; McGuire, J.; Steensgaard, D.B.; Strauss, H.M.; Gram, D.X.; Knudsen, S.M.;

Nielsen, F.S.; Thygesen, P.; Reedtz-Runge, S.; Kruse, T. Discovery of the Once-Weekly Glucagon-Like Peptide-1 (GLP-1) Analogue Semaglutide. *J. Med. Chem.* **2015**, *58*, 7370-7380.

10 Evers, A.; Haack, T.; Lorenz, M.; Bossart, M.; Elvert, R.; Henkel, B.; Stengelin, S.; Kurz, M.; Glien, M.; Dudda, A.; Lorenz, K.; Kadereit, D.; Wagner, M. Design of Novel Exendin-Based Dual Glucagon-like Peptide 1 (GLP-1)/Glucagon Receptor Agonists. *J. Med. Chem.* **2017**, *60*, 4293-4303.

11 Evers, A.; Bossart, M.; Pfeiffer-Marek, S.; Elvert, R.; Schreuder, H.; Kurz, M.; Stengelin, S.; Lorenz, M.; Herling, A.; Konkar, A.; Lukasczyk, U.; Pfenninger, A.; Lorenz, K.; Haack, T.; Kadereit, D.; Wagner, M. Dual Glucagon-like Peptide 1 (GLP-1)/Glucagon Receptor Agonists Specifically Optimized for Multidose Formulations. *J. Med. Chem.* **2018**, *61*, in press.

12 De Graaf, C.; Song, G.; Cao, C.; Zhao, Q.; Wang, M.-W.; Wu, B.; Stevens, R.C. Extending the Structural View of Class B GPCRs. *Trends Biochem. Sci.* **2017**, *42*, 946-960.

13 Wootten, D.; Christopoulos, A.; Sexton, P.M. Emerging Paradigms in GPCR allostery: Implications for Drug Discovery, *Nat. Rev. Drug Discov.* **2013**, *12*, 630-644.

14 Wootten, D.; Savate, E.E.; Valant, C.; May, L.T.; Sloop, K.W. Ficorilli, J.; Showalter, A.D.; Willard, F.S.; Christopoulos, A.; Sexton, P.M. Allosteric Modulation of Endogenous Metabolites as an Avenue for Drug Discovery. *Mol. Pharmacol.* **2012**, *82*, 281-290.

15 Liao, J.; Hong, Y.; Wang, Y.; Von Geldern, T. W.; Zhang, K. E. Phenylalanine Derivatives and Their use as Non-Peptide GLP-1 Receptor Modulators. *WO 2011 094890* and *WO 2011 097300*;

16 Su, H.; He, M.; Li, H.; Liu, Q.; Wang, J.; Wang, Y.; Gao, W.; Zhou, L.; Liao, J.; Young, A.A.; Wang, M.-W. Boc5, a Non-Peptidic Glucagon-Like Peptide-1 Receptor Agonist,

Invokes Sustained Glycemic Control and Weight Loss in Diabetic Mice, *PLoS ONE* **2008**, *3*, e2892.

17 Liu, Q.; Li, N.; Yuan, Y.; Lu, H.; Wu, X.; Zhou, C.; He, M.; Su, H.; Zhang, M.; Wang, J.; Wang, B.; Wang, Y.; Ma, D.; Ye, Y.; Weiss, H.-C.; Gesing, E.R.F.; Liao, J.; Wang, M.-W. Cyclobutane Derivatives as Novel Non-Peptidic Small Molecule Agonists of Glucagon-like Peptide-1 Receptor. *J. Med. Chem.* **2012**, *55*, 250-267.

18 See company website: http://vtvtherapeutics.com/pipeline/ttp273, accessed Feb 22, 2019.

19 Mjalli, A.M.M.; Behme, C.; Christen, D.P.; Polisetti, D.R.; Quada, J.; Santhosh, K.; Bondlela, M.; Guzel, M.; Yarragunta, R.R.; Gohimukkula, D.R.; Andrews, R.C.; Davis, S.T.; Yokum, T.S; Freeman, J.L.R. Substituted azoantracene derivatives, pharmaceutical compositions, and methods of use thereof. *WO 2010 114824.*

20 Almariego, D.; Polisetti, D.R.; Benjamin, E.; El Abdellaoui, H.; Sahoo, S.P. Tris(hydroxymethyl)aminomethane salts of a small-molecule GLP1R agonist and pharmaceutical compositions and uses thereof. *WO 2013 142569*.

21 LOGRA: A Study to Evaluate Safety and Efficacy of TTP273 for 12 Weeks in Subjects With Type 2 Diabetes, NCT02653599. https://clinicaltrials.gov/ct2/show/NCT02653599, accessed Feb 22, 2019.

22 Pfizer company pipeline https://www.pfizer.com/science/drug-product-pipeline- consulted on september 3th 2019.

23 Company pipeline: https://www.lilly.com/discovery/pipeline- Consulted on September 3th. 2019.

24 Kawai, T.; Tanino, F.; Fukazawa, M.; Ogawa, K.; Nagao, S.; Yoshino, H.; Komatsu, S-I.; Suzuki, Y.; Kawabe, Y.; OWL833, an Orally Active Nonpeptide GLP-1 Receptor Agonist, Improves Glucose Tolerance by Increasing Insulin Secretion and Reduces Food Intake of

Cynomolgus Monkeys, American Diabetes Association, 78th Scientific Sessions, New Orlando **2018**, *Poster* 1118.

25 Aspnes. G.E ; Bagley, S.W.; Curto, J. M.; Doivling, M. S.; Edmonds, D.; Flanagan, M. E.; Futatsugi, K-; Griffith, D. A.; Huard, K.; Ingle, G.; Jiao, W.; Limberskis, C.; Ylathiowctz, A.M.; Piotrowski, D.W.; Ruggeri, R.B. GLP1 Agonists and Uses Thereof. *US 2018 0170908*.

26 Yoshino, H.; Tsuchiya, S.; Matsuo, A.; Sato, T.; Nishimoto, M.; Oguri, K.; Ogawa, H.; Nishimura, Y.; Furuta, Y.; Kashiwagi, H.; Hori, N.; Kamon, T.; Shiraishi, T.; Yoshida, S.; Kawai, T.; Tanida, S.; Aoki, M. Pyrazolopyridine Derivative having GLP-1 Receptor Agonist Effect., *WO 2018 056453*.

27 Bueno, A.B.; Showalter, A.D.; Wainscott, D.B.; Stutsman, C.; Marín, A.; Ficorilli, J.; Cabrera, O.; Willard, F.S.; Sloop, K.W. Positive Allosteric Modulation of the Glucagon-like Peptide-1 Receptor by Diverse Electrophiles. *J. Biol. Chem.* **2016**, *291*, 10700-10715.

28 Nolte, W.M.; Fortin, J. P.; Stevens, B.D.; Aspnes, G.E.; Griffith, D.A.; Hoth, L.R.; Ruggeri R. B.; Mathiowetz, A.M.; Limberakis, C.; Hepworth, D.; Carpino, P.A. A Potentiator of Orthosteric Ligand Activity at GLP-1R acts via Covalent Modification. *Nat. Chem. Biol.* **2014**, *10*, 629–631.

29 Corresponding *in-vitro* data are included in the supporting information.

30 Boehm, M.; Martinborough, E.; Moorjani, M.; Tamiya, J.; Huang, L.; Yeager. A. R.; Brahmachary, E.; Fowler, T.; Novak, A; Meghani, P. , Knaags, M.; Novel GLP-1 Receptor Modulators, *WO 2016 015014*.

31 Morris, L.C.; Nance, K.D.; Gentry, P.R.; Days, E.L.; Weaver, C.D.; Niswender, C.M.; Thompson, A.D.; Jones, C.K.; Locuson, C.W.; Morrison, R.D.; Daniels, J.S.; Niswender, K.D.; Lindsley, C.W. Discovery of (S)-2-Cyclopentyl-N-((1-Isopropylpyrrolidin2-yl)-9-methyl-1-oxo-2,9-dihydro-1H-pyrrido[3,4-b]indole-4-carboxamide (VU0453379): a Novel,

CNS Penetrant Glucagon-like Peptide 1 Receptor (GLP-1R) Positive Allosteric Modulator (PAM). *J. Med. Chem.* **2014**, *11*, 10192-10197.

32 Reinhart, G.; Clemons, B.; Desale, H.; Dvorak, L.; Martinborough, E.; Boehm, M.; Peach, R.J.; Scott, F.L. RPC8844 Is a Small Molecule GLP-1R Positive Allosteric Modulator for GLP-1(7-36), GLP-1(9-36) and Oxyntomodulin, and Enhances Glucose-Stimulated Insulin Secretion from Human Pancreatic Islets. American Diabetes Association, 76th Scientific Sessions, New Orleans **2016**, *Poster 1080*.

33 Reinhart, G.; Clemons, B.; Desale, H.; Dvorak, L.; Martinborough, E.; Boehm, M.; Peach, R.J.; Scott, F.L. RPC8844 Is a Small Molecule GLP-1R Positive Allosteric Modulator that Significantly Improves Hyperglycemia and Induces Weight Loss in Type 2 Diabetes Disease Models after Daily Oral Administration, American Diabetes Association, 76th Scientific Sessions, New Orleans **2016**, *Poster* 1107.

34 Rijkelijkhuizen, J.M.; McQuarrie, K.; Girman, C.J.; Stein, P. P.; Mari, A.; Holst, J.J.; Nijpels, G.; Dekker, J-M.; Effects of Meal Size and Composition on Incretin, α-Cell, and β-Cell Responses. *Metabolism* **2010**, *59*, 502-511.

35 Lee, S.-C; Park, S. B. Solid-Phase Parallel Synthesis of Natural Product-like Diaza-bridged Heterocycles through Pictet-Spengler Intramolecular Cyclization. *J. Comb. Chem.* **2006**, *8*, 50-57.

36 Congreve, M., Carr, R., Murray, C., Jhoti, H. A 'Rule of Three' for Fragment-Based Lead Discovery? *Drug Disc. Today* **2003**, *8*, 876–877.

37 For preparation of amine **15**, see supporting information.

38 Eurofins CEREP SA, Le bois l'Evêque, 86600 Celle-Lévescault, France. http://www.eurofins.com, accessed Feb 22, 2019.

39 Full selectivity data given in the supporting information.

40 In our internal assay systems, reference compounds **5** and **6** proved to be inferior in shifting the EC_{50} value for GLP1(9-36)NH_2. See suporting information for corresponding data.

41 Compound **19** showed no effect on the agonistic activity of glucagon on the cAMP accumulation assay on HEK2 cells overexpressing the GLP1-R.

42 This inhibitory effect had also been observed with other isomerically pure compounds from this series, and therefore it was considered unprobable that it arised from one of the diasteroisomers only.

43 Unfortunately, we did not have access to islets of GLP1R(-/-) rats, while *in-vitro* data showed that efficacy of these compounds in recombinant mouse and rat orthologues assays is comparable to the human assay.

44 Jazayeri, A.; Rappas, M.; Brown, A.J.H.; Kean, J.; Errey, J.C.; Robertson, N.J.; Fiez-Vandal, C.; Andrews, S.P.; Congreve, M.; Bortolato, A.; Mason, J.S.; Baig, A.H.; Teobald, I.; Dore, A.S.; Weir, M.; Cooke, R.M.; Marshall, F.H. Crystal Structure of the GLP-1 Receptor Bound to a Peptide Agonist. *Nature* **2017**, *546*, 254-258.

45 Serrano-Vega, M.J.; Magnani, F.; Shibata, Y.; Tate, C.G. Conformational Thermostabilization of the Beta1-Adrenergic Receptor in a Detergent-Resistant Form. *Proc. Natl. Acad. Sci. USA* **2008**, *105*, 877-882.

46 Sherman, W.; Day, T.; Jacobson, M.P.; Friesner, R.A.; Farid, R. Novel Procedure for Modeling Ligand/Receptor Induced Fit Effects. *J. Med. Chem.* **2006**, *49*, 534-553.

47 Wootten, D.; Simms, J.; Miller, L.J.; Christopoulos, A.; Sexton, P.M. Polar Transmembrane Interactions Drive Formation of Ligand-Specific and Signal Pathway-biased Family B G Protein-Coupled Receptor Conformation. *Proc. Natl. Acad. Sci.* **2013**, *110*, 5211-5216.

48 Coopman, K.; Wallis, R.; Robb, G.; Brown, A. J. H.; Wilkinson, G. F.; Timms, D.; Willars, G. B. Residues within the Transmembrane Domain of the Glucagon-Like Peptide-1 Receptor Involved in Ligand Binding and Receptor Activation: Modelling the Ligand-Bound Receptor. *Mol. Endocrinol.* **2011**, *25*, 1804-1818.

49 Zhang, Y.; Sun, B.; Feng, D.; Hu, H.; Chu, M.; Qu, Q.; Tarrasch, J.T.; Li, S.; Kobilka, T.S.; Kobilka, B.K.; Skiniotis, G. Cryo-EM Structure of the Activated GLP-1 Receptor in Complex with a G Protein. *Nature* **2017**, *546*, 248-253.

50 Giacomini, K.M.; Huang, S.M.; Tweedie, D.J.; Benet, L.Z.;Brouwer, K.L.; Chu, X.; Dahlin, A.; Evers, R.; Fischer, V.; Hillgren, K.M.; Hoffmaster, K.A.; Ishikawa, T.; Keppler, D.; Kim, R.B.; Lee, C.A.; Niemi, M.; Polli, J.W.; Sugiyama, Y.; Swaan, P.W.; Ware, J.A.; Wright, S. H.; Yee, S. W.; Zamek-Gliszczynski, M. J.; Zhang, L. Membrane Transporters in Drug Development. *Nature Rev. Drug Discovery 2010*, *9*, 215-236.

51 Kalliokoski, A.; Niemi, M. Impact of OATP Transporters on Pharmacokinetics. *Br. J. Pharmacol.* **2009**, *158*, 693-705.

52 Karlgren, M.; Vildhede, A.; Norinder, U.; Wisniewski, J.R.; Kimoto, E.; Lai, Y.; Haglund, U.; Artursson. P. Classification of Inhibitors of Hepatic Organic Anion Transporting Polypeptides (OATPs): Influence of Protein Expression on Drug−Drug Interactions. *J. Med. Chem.* **2012**, *55*, 4740-4763.

53 Kotsampasakou, E.; Brenner, S.; Jäger, S.; Ecker, G.F.; Identification of Novel Inhibitors of Arganic Anion Transporting Polypeptides 1B1 and 1B3 (PATP1B1 and OATP1B3) Using a Consensus Vote of Six Classification Models. *Mol. Pharm.* **2015**, *12*, 4395-4404.

54 Matter, H.; Buning, C.; Giegerich, C. Unpublished results.

55 Sharom, F.J. ABC Multidrug Transporters: Structure, Function and Role in Chemoresistance. Pharmacogenomics, 2008, 9, 105-127.

56 Aller, S.G.; Yu, J.; Ward, A.; Wenig, Y.; Chittaboina, S.; Zhuo, R.; Harrell, P.M.; Trinh, Y.T.; Zhang, Q.; Urbatsch, I.L.; Chang, G. Structure of P-Glycoprotein Reveals a Molecular Basis for Poly-Specific Drug Binding. *Science* **2009**, *323*, 1718-1722.

57 Nies, AT.; Schwab, M; Keppler, D. Interplay of Conjugating Enzymes with OATP Uptake Transporters and ABCC/MRP Efflux Pumps in the Elimination of Drugs. *Exp. Opin. Drug Metab. Toxicol*. **2008**, *4*, 545-568.

58 Imaoka, T.; Mikkaichi, T.; Abe, K.; Hirouchi, M.; Okudaira, N.; Izumi, T. Integrated Approach of in Vivo and in Vitro Evaluation of the Involvement of Hepatic Uptake Organic Anion Transporters in the Drug Disposition in Rats using Rifampicin as an Inhibitor. *Drug Metab. Disp.* **2013**, *41*, 1442-1449.

59 Shingaki, T.; Takashima, T.; Ijuin, R.; Zhang, X.; Onoue, T.; Katayama, Y.; Okauchi, T.; Hayashinaka, E.; Cui, Y.; Wada, Y.; Suzuki, M.; Maeda, K.; Kusuhara, H.; Sugiyama, Y.; Watanabe, Y. Evaluation of Oatp and Mrp2 Activities in Hepatobiliary Excretion Using Newly Developed Positron Emission Tomography Tracer [^{11}C]Dehydropravastatin in Rats. *J. Pharmacol. Exp. Therap.* **2013**, *347*, 193-202.

60 Wang, H.; Sun, P.; Wang, C.; Meng, Q.; Liu, Z.; Huo, X.; Sun, H.; Ma, X.; Peng, J.; Liu, K. Liver Uptake of Cefditoren is Mediated by OATP1B1 and OATP2B1 in Humans and Oatp1a1, Oatp1a4, and Oatp1b2 in Rats. *RSC Advances* **2017**, *7*, 30038-30048.

61 Zhao, D.; Gao, Z.-D.; Han, D.; Li, N.; Zhang, Y.-J.; Lu, Y.; Li, T.-T; Chen, X.-HJ. Influence of Rifampicin on the Pharmacokinetics of Salvianolic Acid B May Involve Inhibition of Organic Anion Transporting Polypeptide (Oatp) Mediated Influx. *Phytotherapy Res.* **2012**, *26*, 118-121.

62 Lyons, M.A.; Reisfeld, B.; Yang, R.S.H.; Lenaerts, A.J. A Physiologically Based Pharmacokinetic Model of Rifampin in Mice. *Antimicrob. Agents Chemother.* **2013**, *57*, 1763-1771.

63 Irwin, N.; McClean, P.L.; Cassidy, R.S.; O'Harte, F.P.; Green, B.D.; Gault, V.A.; Harriott, P.; Flatt, P.R. Comparison of the Anti-Diabetic Effects of GIP- and GLP1-Receptor Activation in Obese Diabetic (ob/ob) Mice: Studies with DPP IV resistant N-AcGIP and exendin(1- 39)amide. *Diabetes/Metabolism Res. Rev.* **2007**, *23*, 572-579.

64 Miyazaki, J.; Araki, K.; Yamato, E.; Ikegami, H.; Asano, T.; Shibasaki, Y.; Oka, Y.; Yamamura, K. Establishment of a Pancreatic Beta Cell Line that Retains Glucose Inducible Insulin Secretion: Special Reference to Expression of Glucose Transporter Isoforms. *Endocrinology* **1990**, *127*, 126-132.

65 Artursson, P.; Karlsson, J. Correlation between Oral Drug Absorption in Humans and Apparent Drug Permeability Coefficients in Human Intestinal Epithelial (Caco-2) Cells. *Biochem. Biophys. Res. Comm.* **1991**, *175*, 880–885.

66 Borchardt, R.T.; Freidinger, R.M.; Sawyer, T.K. *Integration of Pharmaceutical Discovery and Development*, Plenum Press, New York (US), 1998.

67 Hidalgo, I.J.; Raub, T.J.; Borchardt, R.T. Characterization of the Human Colon Carcinoma Cell line (Caco-2) as a Model System for Intestinal Epithelial Permeability. *Gastroenterology* **1989**, *96*, 736–749.

68 Artursson, P. Epithelial Transport of Drug in Cell Culture. I: a Model for Studying the Passive Diffusion of Drugs over Intestinal Absorptive (Caco-2) cells. *J. Pharm. Sci*. **1990**, *79*, 476–82.

69 Dudda, A.; Kürzel, G.U. Metabolism Studies *in vitro* and *in vivo*. Chapter II.H. In: *Drug Discovery and Evaluation: Safety and Pharmacokinetic Assays*. Vogel, H.G.; Hock, F.J.; Maas, J.; Mayer, D. (Eds.), Springer, Berlin/New York, 2006, pp 493–520.

70 U.S. Department of Health and Human Services. Food and Drug Administration. Center for Drug Evaluation and Research, Guidance for industry: Drug Interaction Studies - Study Design, Data Analysis and Implications for Dosing and Labeling Recommendations, Draft Guidance 2012.

71 EMA, Guideline on the Investigation of Drug Interactions, Draft Guideline 2010.

72 EMA, Guideline on the Investigation of Drug Interactions, 2013.

73 Guengerich, F.P. Cytochrome p450 and Chemical Toxicology. *Chem. Res. Toxicol*. **2008**, *21*, 70–83.

74 Obach, R.S.; Walsky, R.L.; Venkatakrishnan, K. The Utility of *in Vitro* Cytochrome P450 Inhibition Data in the Prediction of Drug-Drug Interactions. *J. Pharmacol. Exp. Ther.* **2006**, *316*, 336–348.

75 Obach, R.S.; Robert, L.W.; Venkatakrishnan, K. Mechanism-Based Inactivation of Human Cytochrome P450 Enzymes and the Prediction of Drug-Drug interactions. *Drug Metab Dispos*, **2007**, *35*, 246–255.

76 Zhang, L.; Zhang, Y.D.; Zhao, P.; Shiew-Mei, H. Predicting Drug–Drug Interactions: An FDA Perspective, *Am. Assoc. Pharm. Sci. J.* **2009**, *11*, 300–306.

77 Grimm, S.W.; Einolf, H.J.; Hall, S.D.; He, K.; Lim, H.K.; Ling, K.-H.; Lu, C.; Nomeir, A.A.; Seibert, E.; Skordos, K.W.; Tonn, G.R.; Horn, R.V.; Wang, R.W.; Wong, Y.N.; Yang, T.J.; Obach, R.S., The Conduct of *in Vitro* Studies to Address Time-Dpendent Inhibition of Drug Metabolizing Enzymes: A Perspective of the Pharmaceutical Research and Manufacturers of America, *Drug Metab. Disp.* **2009**, *37*, 1355–1370.

78 Grime, K.H.; Bird, J.; Ferguson, D.; Riley, R.J. Mechanism-Based Inhibition of Cytochrome P450 Enzymes: an Evaluation of Early Decision Making *in vitro* Approaches and Drug–Drug Interaction Prediction Methods. *Eur. J. Pharm. Sci.* **2009**, *36*, 175–191.

79 Mukadam, S.; Tay, S.; Tran, D.; Wang, L.M.; Delarosa, E.; Cyrus, K.S.S.; Halladay, J.R.; Kenny, J. Evaluation of Time-Dependent Cytochrome P450 Inhibition in a High-Throughput, Automated Assay: Introducing a Novel Area Under the Curve Shift Approach. *Drug Metab. Lett.*, **2012**, *6*, 43–53.

80 Ogilvie, B.W.; Usuki, E.; Yerino, P.; Parkinson, A. *In Vitro* Approaches for Studying the Inhibition of Drug-Metabolizing Enzymes Responsible for the Metabolism of Drugs (Reaction Phenotyping) with Emphasis on Eytochrome P450. In: *Drug-Drug Interactions*, Drugs and thePharmaceutical Sciences, 2nd edition, Volume 179. Rodrigues, A.D. (Ed.), Informa Healthcare, New York (US), 2011, pp 231–358.

81 (a) Urso, R.; Blardi, P.; Giorgi, G. A short introduction to pharmacokinetics. *Eur. Rev. Med. Pharmacol. Sci.* **2002**, *6*, 33–44. (b) Ritschel, W.A.; Kearns, G.L. Handbook of Basic Pharmacokinetics, 6th edition; APhA: Washington, DC, U.S., 2004. (c) Food and Drug Administration. Additional Studies part B. Metabolism and Pharmacokinetic Studies, 1993 Draft "Redbook II". Guidance for Industry and Other Stakeholders Toxicological Principles for the Safety Assessment of Food Ingredients. Redbook 2000 (Revised 2007). http://www.fda.gov/downloads/Food/GuidanceRegulation/UCM078741.pdf, accessed Feb 22, 2019.

82 Schrödinger molecular modeling suite, release 2018-1: Schrödinger LLC: New York, NY, 2018.

83 PDB files from RCSB Protein Database: http://www.rcsb.org/pdb, accessed Feb 22, 2019.

a) Bernstein, F.C.; Koetzle, T.F.; Williams, G.J.B.; Meyer, E.F.; Brice, M.D.; Rodgers, J.R.; Kennard, O.; Shimanouchi, T.; Tasumi; M. The Protein Data Bank: a Computer-Based Archival File for Macromolecular Structures. *J. Mol. Biol.* **1977**, *112,* 535-542.

b) Berman**,** J.W.; Zukang, F.; Gilliland, G.; Bhat, T.N.; Weissig, H.; Shindyalov, I.N.; Bourne, P.E. The Protein Data Bank. *Nucl. Acids Res.* **2000**, *28*, 235-242.

84 Sastry, G.M.; Adzhigirey, M.; Day, T.; Annabhimoju, R.; Sherman, W. Protein and Ligand Preparation: Parameters, Protocols, and Influence on Virtual Screening Enrichments. *J. Comput.-Aided Mol. Des.* **2013**, *27*, 221-234.

85 Shivakumar, D.; Harder, E.; Damm, W.; Friesner, R.A.; Sherman, W. Improving the Prediction of Absolute Solvation Free Energies Using the Next Generation OPLS Force Field. *J. Chem. Theory Comput.* **2012**, *8*, 2553-2558.

86 Harder, E.; Damm, W.; Maple, J.; Wu, C.; Reboul, M.; Xiang, J.Y.; Wang, L.; Lupyan, D.; Dahlgren, M.K.; Knight, J.L.; Kaus, J.W.; Cerutti, D.S.; Krilov, G.; Jorgensen, W.L.; Abel, R.; Friesner, R.A. OPLS33: A Force Field Providing Broad Coverage of Drug-Like Small Molecules and Proteins. *J. Chem. Theory Comput.* **2016**, *12*, 281-296.

87 Baringhaus, K.-H.; Hessler, G.; Matter, H.; Schmidt, F. Development and Applications of Global ADMET Models: In Silico Prediction of Human Microsomal Lability. In *Chemoinformatics for Drug Discovery*, Bajorath, J. (Ed.), Wiley, Hoboken, NJ, 2014, pp 245-265.

88 Matter, H.; Anger, L.T.; Giegerich, C.; Güssregen, S.; Hessler, G.; Baringhaus, K.-H. Development of in Silico Filters to Predict Activation of the Pregnane X Receptor (PXR) by Structurally Diverse Drug-Like Molecules. *Bioorg. Med. Chem.* **2012**, *20*, 5352-5365.

89 Sadowski, J.; Rudolph, C.; Gasteiger, J. The Generation of 3D-Models of Host-Guest Complexes. *Anal. Chim. Acta* **1992**, *265*, 233-241.

90 Corina (version 3.491). Available from Molecular Networks Inc., Erlangen, Germany.

91 MOE (version 2011). Available from Chemical Computing Group (CCG), Montreal, Canada.

92 Schneider, G.; Neidhart, W.; Giller, T.; Schmidt, G. "Scaffold-Hopping" by Topological Pharmacophore Search: A Contribution to Virtual Screening. *Angew. Chem. Int Ed.* **1999**, *38*, 2894-2896.

93 Ghose, A.K.; Crippen, G.M. Atomic Physicochemical Parameters for Three-Dimensional-Structure-Directed Quantitative Structure-Activity Relationships. 2. Modeling Dispersive and Hydrophobic Interactions. *J. Chem. Inf. Comput. Sci.* **1987**, *27*, 21-35.

94 Quinlan, J.R. Improved Estimates for the Accuracy of Small Disjuncts. *Machine Learn.* **1991**, *6*, 93-98.

95 Quinlan, J.R. Learning with Continuous Classes. In: *Proc. AI'92, 5th Australian Joint Conference on Artificial Intelligence*, Adams, A.; Sterling, L. (Eds.), World Scientific, Singapore, **1992**, 343-348.

96 Quinlan, J.R. Combining Instance-Based and Model-Based Learning. In: Proceedings ML'93 (Utgoff, P.E. Ed.), Morgan Kaufmann, Los Altos, CA, 1993.

97 Z. Wang, Y. Chen, H. Liang, A. Bender, R.C. Glen, A. Yan. P-glycoprotein Substrate Models using Support Vector Machines Based on a Comprehensive data set. *J. Chem. Inf. Model.* **2011**, *51*, 1447-1456.

Table of Contents Graphic